Phenyl 2-Pyridyl Ketone and Its Oxime in Manganese Carboxylate Chemistry: Synthesis, Characterisation, X-ray Studies and Magnetic Properties of Mononuclear, Trinuclear and Octanuclear Complexes

Constantinos J. Milios,[a] Theocharis C. Stamatatos,[a] Panayotis Kyritsis,[b] Aris Terzis,[c] Catherine P. Raptopoulou,[c] Ramon Vicente,*[d] Albert Escuer,*[d] and Spyros P. Perlepes*[a]

The use of phenyl 2-pyridyl ketone [(ph)(2-py)CO] and its oxime [(ph)(2-py)CNOH] in manganese benzoate chemistry has been investigated. The reaction of an excess of (ph)(2-py)CNOH with $Mn(O_2CPh)_2 \cdot 2H_2O$ affords the mononuclear complex $[Mn^{II}(O_2CPh)_2\{(ph)(2-py)CNOH\}_2] \cdot 1.2H_2O$ ($1 \cdot 1.2H_2O$) in high yield. The Mn^{II} ion is coordinated by two monodentate benzoates and two N,N'-bidentate chelating (ph)(2-py)CNOH molecules in a *cis-cis-trans* fashion. The comproportionation reaction between $Mn(O_2CPh)_2 \cdot 2H_2O$ and $NnBu_4MnO_4$ (3:1) in the presence of (ph)(2-py)CNOH in $MeCN/EtOH/CH_2Cl_2$ leads to the isolation of the mixed-valent cluster $[Mn_8O_2(OH)_2(O_2CPh)_{10}\{(ph)(2-py)CNO\}_4] \cdot 4CH_2Cl_2$ ($2 \cdot 4CH_2Cl_2$) in about 55% yield. A second synthetic procedure that leads to pure **2** involves the reaction between the known starting material $(NnBu_4)[Mn_4^{III}O_2(O_2CPh)_9(H_2O)]$ and four equivalents of the oxime ligand in CH_2Cl_2. The centrosymmetric octanuclear molecule contains four Mn^{II} and four Mn^{III} ions held together by two μ_4-O^{2-} ligands and two μ_3-OH^- ions to give the unprecedented $[Mn_8(\mu_4\text{-}O)_2(\mu_3\text{-}OH)_2]^{14+}$ core, with peripheral ligation provided by ten $PhCO_2^-$ (two η^1, four *syn,syn* η^1:η^1:μ_2 and four η^1:η^2:μ_3) and four η^1:η^1:η^1:μ_2 (ph)(2-py)CNO$^-$ ions. The 1:1 reaction between $Mn(O_2CPh)_2 \cdot 2H_2O$ and the ketone (ph)(2-py)CO affords the trinuclear complex $[Mn_3(O_2CPh)_6\{(ph)(2-py)CO\}_2]$ (**3**) in more than 80% yield. As judged from single-crystal X-ray crystallography, the complex adopts a linear structure with one η^1:η^2:μ_2 and two η^1:η^1:μ_2 benzoates spanning each pair of metal ions. The terminal Mn^{II} ions are capped by bidentate chelating (ph)(2-py)CO ligands. The three complexes have been characterised by IR spectroscopy. The CV study of complex **2** in CH_2Cl_2 reveals irreversible reduction and oxidation processes. The magnetic properties of **2** and **3** have been studied by variable-temperature dc magnetic-susceptibility techniques. As the temperature approaches zero, the value of the $\chi_M T$ product for **2** approaches zero and, thus, the octanuclear complex has an $S = 0$ ground state. This $S = 0$ ground state is explained in terms of the magnetic behaviour of the central, butterfly-like $[Mn_4^{III}(\mu_3\text{-}O)_2]^{8+}$ sub-core. The results for **3** reveal weak antiferromagnetic coupling, with $J = -2.7$ cm^{-1} for adjacent Mn^{II} ions.
(© Wiley-VCH Verlag GmbH & Co. KGaA, 69451 Weinheim, Germany, 2004)

Introduction

There are several reasons why manganese carboxylate chemistry is the focus of such great research interest at present. One such reason is that a tetranuclear Mn carboxylate cluster is an integral component of the photosystem II reaction centre of green plants (and cyanobacteria), where it is responsible for the light-driven oxidation of water to dioxygen gas.[1] This Mn_4 water oxidation complex (WOC) is the site of substrate (water) binding, deprotonation and oxidative coupling to O_2, although the exact structure of the cluster[2] and its precise mechanism[1] of action are currently unknown. The synthesis and structural/spectroscopic characterisation of Mn model complexes[1,3] have provided a wealth of data for comparison and contrast with the corresponding characteristics for the native WOC. In the last ten years, the synthesis and study of polynuclear Mn carboxylate complexes have also been stimulated by the discovery that some of them exhibit the new magnetic phenomenon of single-molecule magnetism.[4] This property is the ability of discrete molecules to exhibit the superparamagnet-like property of slow magnetisation relaxation and thus to behave as magnets below their blocking temperature by exhibiting magnetisation vs. field hysteresis. Such properties do not arise from intermolecular exchange interactions and long-range ordering, but instead from a combination of two intramolecular properties, namely a

[a] Department of Chemistry, University of Patras,
265 04 Patras, Greece
E-mail: perlepes@patreas.upatras.gr
[b] Department of Chemistry, University of Athens,
15771 Athens, Greece
E-mail: kyritsis@chem.uoa.gr
[c] Institute of Materials Science, NCSR "Demokritos",
15310 Aghia Paraskevi Attikis, Greece
[d] Departament de Quimica Inorganica, Universitat de Barcelona,
Diagonal 647, 08028 Barcelona, Spain
E-mail: ramon.vicente@qi.ub.es and albert.escuer@qi.ub.es

large ground-state spin (S) and a significant magnetoanisotropy of the Ising (easy-axis) type, the latter being reflected in a large and negative value of the zero-field splitting parameter D.[4] The first single-molecule magnet (SMM) was [Mn$_{12}$O$_{12}$(O$_2$CMe)$_{16}$(H$_2$O)$_4$], which possesses an $S = 10$ ground state,[5] and a number of other Mn$_x$ carboxylate SMMs have since been discovered.[4,6] There is thus a continuing need to develop new synthetic methods for the preparation of new polynuclear Mn carboxylate compounds.

Among the many synthetic lines currently being pursued by our groups and others in this field is the reaction of a bridging ligand containing both chelating sites and ionizable hydrogens with a simple Mn carboxylate "salt" or a preformed Mn carboxylate cluster that does not already incorporate any chelating ligand.[6,8] As long as the RCO$_2^-$/bridging ligand ratio is high enough to leave an amount of non-protonated RCO$_2^-$ ions in the reaction mixture, this approach normally leads to heteroleptic RCO$_2^-$/deprotonated bridging ligand metal clusters. One of the ligands that has previously proved to be useful in these syntheses, giving many new polynuclear complexes, is di-2-pyridyl ketone [(2-py)$_2$CO; Figure 1]. Our groups have been exploring "ligand blend" reactions involving the monoanion (2-py)$_2$C(OH)O$^-$ or the dianion (2-py)$_2$CO$_2^{2-}$ of the *gem*-diol form of (2-py)$_2$CO (these anions are stabilized *only* in the presence of metal ions[8]) *and* carboxylates. These reaction schemes have led[9] to a variety of Fe, Co, Ni, Cu, Zn clusters with nuclearities ranging from three to twelve and with interesting magnetic properties, including SMM behaviour.[9j] In Mn carboxylate chemistry the most impressive cluster isolated[10] is [Mn$_{10}^{II}$Mn$_4^{III}$O$_4$(O$_2$CMe)$_{20}${(2-py)$_2$C(OH)O}$_4$]; the observed tetradecanuclearity is extremely rare in 3d-metal chemistry. Recently we have extended our efforts to ligands (Figure 1) that present a structural similarity to (2-py)$_2$CO; our goals are to investigate to what extent the use of such ligands might affect the identity of the obtained products compared with (2-py)$_2$CO and to what extent this might thus prove to be a route to new cluster types. Our initial work was concentrated on di-2-pyridyl ketone oxime, (2-py)$_2$CNOH, a ligand whose employment

in Mn carboxylate chemistry gave the new family of valence-trapped, mixed-valence complexes[11] [Mn$_2^{II}$Mn$_2^{III}$-(O$_2$CR)$_2$X$_2${(2-py)$_2$CNO}$_2${(2-py)$_2$CO$_2$}$_2$], where X$^-$ is Cl$^-$, Br$^-$ or RCO$_2^-$; it has been of great interest that an appreciable quantity of the oxime ligand undergoes transformation to yield the coordinated dianion of the *gem*-diol form of (2-py)$_2$CO. The mechanism of this transformation probably involves reaction(s) of the electrophilically activated coordinated oxime group. In attempting to extend the above-mentioned chemistry, and to create new topologies, we have begun reactions featuring phenyl 2-pyridyl ketone oxime, (ph)(2-py)CNOH, and its ketone, (ph)(2-py)CO. These ligands have different electronic properties to those of (2-py)$_2$CNOH and (2-py)$_2$CO, respectively, and have never been employed in polynuclear 3d-metal chemistry.

Herein we describe our efforts toward the use of (ph)(2-py)CNOH and (ph)(2-py)CO in Mn benzoate chemistry. In particular, we report the synthesis, structure and characterisation of one mononuclear Mn^{II} complex, one trinuclear Mn^{II} complex and one octanuclear Mn$^{II/III}$ cluster featuring a novel core. A small portion of this work has been communicated previously.[10] There is currently a renewed interest in the coordination chemistry of oximes.[12] This interest is driven by a number of considerations.[12,13] In contrast to the great number of studies concerning metal complexes of single oximes and salicylaldoxime, little is known[12,13] about complexes of pyridyloximes, although this class of compounds could offer unique features in terms of structural and physical properties.

Results and Discussion

Synthesis

The initial reaction explored was that between Mn(O$_2$CPh)$_2$·2H$_2$O and one equivalent of (ph)(2-py)CNOH in MeCN/EtOH. The pale-orange solution obtained gradually turned brown due to slow oxidation of Mn^{II} under the normal laboratory atmosphere. Evaporation of the resulting solution under reduced pressure, redissolv-
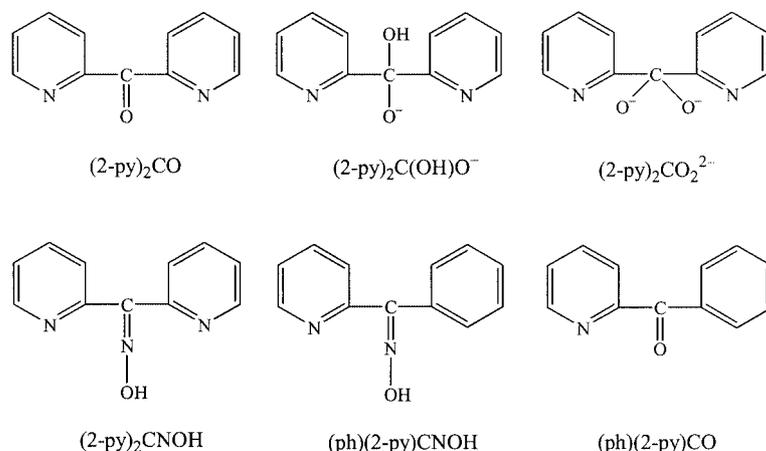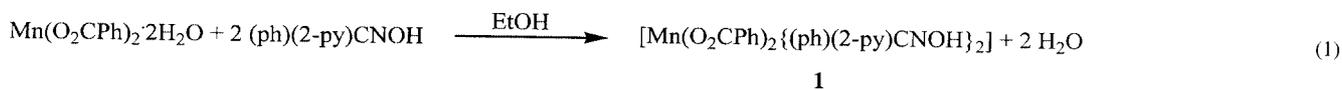

Figure 1. Some of the ligands discussed in the text; note that (2-py)$_2$C(OH)O$^-$ and (2-py)$_2$CO$_2^{2-}$ do not exist as free species — they exist only in their metal complexes

$$Mn(O_2CPh)_2 \cdot 2H_2O + 2\ (ph)(2\text{-}py)CNOH \xrightarrow{\text{EtOH}} [Mn(O_2CPh)_2\{(ph)(2\text{-}py)CNOH\}_2] + 2\ H_2O$$
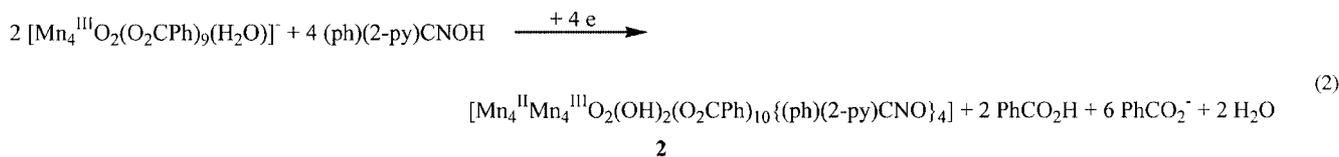
1   (1)

ing the residue in CH_2Cl_2 and layering the solution with Et_2O/n-hexane gave a mixture of yellow and dark-brown crystals, which were readily separated manually and crystallographically identified as $[Mn(O_2CPh)_2\{(ph)(2\text{-}py)CNOH\}_2]\cdot1.2H_2O$ ($1\cdot1.2H_2O$) and $[Mn_8O_2(OH)_2(O_2CPh)_{10}\{(ph)(2\text{-}py)CNO\}_4]\cdot4CH_2Cl_2$ ($2\cdot4CH_2Cl_2$), respectively. The latter is a mixed-valence ($4Mn^{II}$, $4Mn^{III}$) complex (vide infra). With the identities of **1** and **2** established, alternative and convenient syntheses of pure materials were sought. The mononuclear product contains a (ph)(2-py)CNOH/Mn ratio of 2:1, whereas the reaction solution had a ratio of 1:1; thus, attempts to obtain pure **1** were made by increasing the ligand/Mn reaction ratio. The preparation of pure **1** *under aerobic conditions* was achieved by the reaction of $Mn(O_2CPh)_2\cdot2H_2O$ with an excess of oxime in EtOH [Equation (1)].
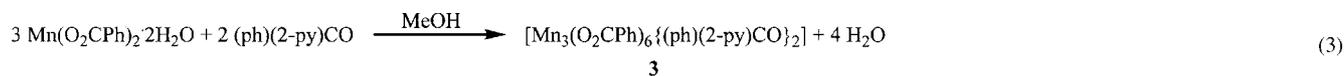
Two procedures were developed that lead to preparation of pure **2**. The first one involves a comproportionation reaction between $Mn(O_2CPh)_2\cdot2H_2O$ and $NnBu_4MnO_4$ [14] in a 3:1 ratio in the presence of (ph)(2-py)CNOH. This ratio, on paper, gives an average Mn oxidation state in solution of $Mn^{+3.25}$, higher than that ($Mn^{+2.5}$) observed in solid **2**. The source of the reducing agent is probably EtOH from the solvent mixture, solvent impurities or excess ligand groups, facilitated by the strongly oxidizing nature of Mn^{III}.[15] It is also likely, as with many other reactions in higher oxidation state Mn chemistry, that the reaction solution contains a complicated mixture of several species in equilibrium, with factors such as relative solubility, lattice energies, crystallisation kinetics and others determining the identity of the isolated product.[16] Comproportionation reactions between Mn^{II} and Mn^{VII} sources have found extensive use to produce $Mn/O^{2-}/RCO_2^-$ clusters of various nuclearities.[15,16] Complex **2** was isolated from the above reaction solution in 55% yield. In an attempt to increase further the yield of the product, the Mn^{II}/MnO_4^- ratio was increased to that which would give an average Mn oxidation state of +2.5, as found in **2**, but this instead led to crystallisation of $[Mn_6O_2(O_2CPh)_{10}(MeCN)_4]$[17a] and/or $[Mn_6O_2(O_2CPh)_{10}(EtOH)_4(H_2O)]\cdot EtOH$[17b] containing $4Mn^{II}$, $2Mn^{III}$, and no bound (ph)(2-py)CNO$^-$ groups. These and similar hexanuclear species differing in the identity of the bound neutral monodentate ligands have been previously observed and are common products at this oxidation level with benzoate groups.[17c] Attempts to obtain clusters with higher average

Mn oxidation states were also made by decreasing the Mn^{II}/MnO_4^- ratio; for example, a ratio of 3:2 (this ratio on paper gives an average Mn oxidation state in solution of Mn^{4+}) again resulted in the isolation of **2** in low (< 30%) yields. The second procedure that leads to pure **2** involves the conversion of $(NnBu_4)[Mn_4O_2(O_2CPh)_9(H_2O)]$ into a higher nuclearity product. The anion $[Mn_4O_2(O_2CPh)_9(H_2O)]^-$ contains only Mn^{III} ions, and only $PhCO_2^-$ and H_2O peripheral ligation.[15] The latter fact makes it especially useful for synthesising higher nuclearity products: it has, for example, permitted the isolation of $(NnBu_4)[Mn_8O_6Cl_6(O_2CPh)_7(H_2O)_2]$,[18a] $(NnBu_4)[Mn_8O_4(O_2CPh)_{12}(Et_2mal)_2(H_2O)_2]$[15] ($Et_2malH_2$ = 2,2-diethylmalonic acid) and $K_4[Mn_{18}O_{16}(O_2CPh)_{22}(phth)_2(H_2O)_4]$[18b] ($H_2phth$ = phthalic acid) when treated with Me_3SiCl, $Na_2(Et_2mal)$ and $KH(phth)$, respectively. Treatment of complex $(NnBu_4)[Mn_4O_2(O_2CPh)_9(H_2O)]$ with four equivalents of (ph)(2-py)CNOH in CH_2Cl_2 leads to subsequent isolation of pure crystalline **2** in acceptable yield (ca. 30%). The formation of **2** by this route can be summarised in Equation (2).

It seems that the core of **2** can be thought of as being derived from the "butterfly" $[Mn_4(\mu_3\text{-}O)_2]^{8+}$ core[15] of the starting tetranuclear material by dimerisation/reduction / protonation steps (the order is arbitrary). The $4Mn^{II}$, $4Mn^{III}$ description of **2** requires the reduction of four Mn^{III} ions to have occurred; as stated above, it is not uncommon to find Mn^{III} — a strong oxidizing agent — being reduced by ligand groups, solvent impurities, etc.[15] An alternative means for the generation of the Mn^{II} ions in **2** is disproportionation of Mn^{III}, in which case Mn^{IV}-containing species would be in the filtrate.[15] We have not attempted to identify the exact origin of the Mn^{II} ions in the product, nor would it be a simple matter to do so. The excess of (ph)(2-py)CNOH (oxime/Mn_4 = 4:1) is beneficial to the preparation, because use of a stoichiometric amount (oxime/Mn_4 = 2:1) yields an oxime-free product analysed as $[Mn_6O_2(O_2CPh)_{10}(H_2O)_x]$ (x = 2−3).

The structure of **2** was shown by crystallography (vide infra) to contain an octanuclear core in which two $[Mn_4(\mu_3\text{-}O)(\mu_3\text{-}OH)]$ units have been linked together. Although **2** is a new and interesting complex, the question that arose after its characterisation was whether a discrete tetranuclear product containing this unit might be attainable by suitable alteration of the reaction conditions. A number of such at-

$$2\ [Mn_4^{III}O_2(O_2CPh)_9(H_2O)]^- + 4\ (ph)(2\text{-}py)CNOH \xrightarrow{+4\ e}$$

(2)

$$[Mn_4^{II}Mn_4^{III}O_2(OH)_2(O_2CPh)_{10}\{(ph)(2\text{-}py)CNO\}_4] + 2\ PhCO_2H + 6\ PhCO_2^- + 2\ H_2O$$

2

$$3 \ Mn(O_2CPh)_2 \cdot 2H_2O + 2 \ (ph)(2\text{-}py)CO \xrightarrow{MeOH} [Mn_3(O_2CPh)_6\{(ph)(2\text{-}py)CO\}_2] + 4 \ H_2O \tag{3}$$
$$\textbf{3}$$

tempts were made, but with no successful isolation of any other species; in particular, increasing the (ph)(2-py)CNOH/Mn₄ reaction ratio further still gives complex **2** as the isolable product. Thus, complex **2** remains the only polynuclear Mn/PhCO₂⁻/(ph)(2-py)CNO⁻ species to have been identified to date.

The next goal of this work was to synthesise Mn complexes of the ketone of (ph)(2-py)CNOH, i.e., (ph)(2-py)CO (Figure 1). The reaction used to prepare the trinuclear manganese(II) complex [Mn₃(O₂CPh)₆{(ph)(2-py)CO}₂] (**3**) is shown in Equation (3).

The "wrong" reaction ratio employed experimentally (Mn/ketone = 1:1), compared to the stoichiometric ratio (Mn/ketone = 1.5:1) required by Equation (3), obviously did not prove detrimental to the isolation of the trinuclear product. We have not explored reactions in any solvent (complex **3** can be isolated from a variety of solvents including EtOH, MeCN and CH₂Cl₂) using Mn^{II}:(ph)(2-py)CO ratios other than 1:1.

Attempts to oxidize one or more Mn^{II} ions of **3** failed to give a crystalline compound. Several 3:1 and 3:2 **3**/NnBu₄MnO₄ reaction mixtures were studied under various conditions, but almost all led to a mixture of the starting trinuclear complex and an as-yet unidentified reddish, non-crystalline material; we did not study this material further. Thus, complex **3** does not appear promising for the isolation of other (possibly larger) Mn clusters. We also investigated in situ reactions between Mn(O₂CPh)₂·2H₂O and (ph)(2-py)CO in the presence of NnBu₄MnO₄ at various Mn^{II}/Mn^{VII} ratios, but, somewhat to our surprise, the only isolable product remained complex **3**, thus proving the great thermodynamic stability of the [Mn₃^{II}(η¹:η¹:μ₂-O₂CR)₄(η¹:η²:μ₂-O₂CR)₂] core. Along these lines, it is worth noting that reactions of the preformed, mixed-valence compound [Mn₃^{II,III,III}O(O₂CPh)₆(py)₂(H₂O)][19] (py = pyridine) and (ph)(2-py)CO led to fading of the reaction solutions and subsequent isolation of **3**.

X-ray Crystal Structures

[Mn(O₂CPh)₂{(ph)(2-py)CNOH}₂]·1.2H₂O (1·1.2H₂O)

A labelled plot of the structure of the mononuclear compound **1** is shown in Figure 2. Selected bond lengths and angles are listed in Table 1. The structure consists of well-separated [Mn(O₂CPh)₂{(ph)(2-py)CNOH}₂] moieties and solvate H₂O molecules. The Mn^{II} atom is coordinated by two monodentate benzoates and two N,N'-bidentate chelating (ph)(2-py)CNOH molecules. The six-coordinate molecule is the *cis-cis-trans* isomer considering the positions of the oxygen, pyridyl nitrogen and oxime nitrogen atoms, respectively. An analogous *cis-cis-trans* arrangement has also been observed in the molecular structure of [Mn(O₂CCF₃)₂{(py)CHNOH}₂],[13] where (py)CHNOH is 2-pyridinealdoxime. The molecule has no imposed sym-
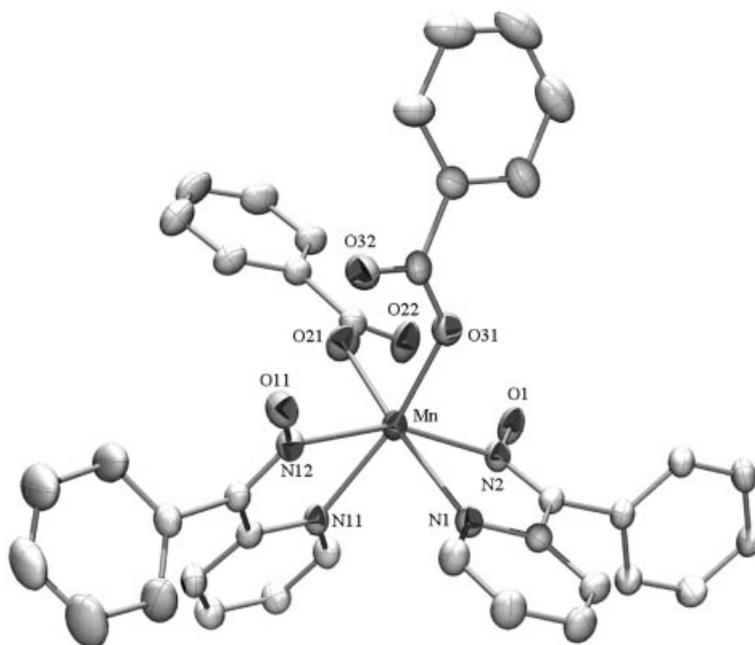

Figure 2. ORTEP plot of the molecule of complex **1**·1.2H₂O at the 30% probability level

metry, although it approximates closely to C_2 symmetry, with the C_2 axis bisecting the O(21)−Mn−O(31) angle. The four Mn−N bond lengths [2.255(3)−2.319(4) Å] are similar. The distortion from a perfect octahedral geometry is primarily a consequence of the small bite-angle of the chelating ligands, which leads to acute N(1)−Mn−N(2) and N(11)−Mn−N(12) angles of 70.6(1)° and 70.8(1)°, respectively. There are two strong intramolecular hydrogen bonds with the uncoordinated oxime oxygens as donors and the "free" carboxylate oxygens as acceptors. Their dimensions are: O(1)···O(22) 2.524 Å, H(O1)···O(22) 1.735 Å, O(1)−H(O1)···O(22) 169.4° and O(11)···O(32) 2.532 Å,

H(O11)···O(32) 1.519 Å, O(11)−H(O11)···O(32) 153.1°. The existence of these strong hydrogen bonds most likely explains the isolation of the *cis-cis-trans* isomer.

[Mn₈O₂(OH)₂(O₂CPh)₁₀{(ph)(2-py)CNO}₄]·4CH₂Cl₂ (2·4CH₂Cl₂)

A partially labelled plot of the octanuclear complex **2** is shown in Figure 3. Selected interatomic distances and angles are listed in Table 2. Complex **2**·4CH₂Cl₂ crystallises in the monoclinic space group C2/c. Its structure consists of the octanuclear [Mn₈O₂(OH)₂(O₂CPh)₁₀{(ph)(2-py)CNO}₄] moiety and solvate CH₂Cl₂ molecules; the latter will not be further discussed. The molecule lies on an inversion centre; it comprises eight Mn ions held together by two μ_4-O²⁻ ions [O(21), O(21′)] and two μ_3-OH⁻ ions [O(22), O(22′)] to give a [Mn₈(μ_4-O)₂(μ_3-OH)₂]¹⁴⁺ core, with peripheral ligation provided by ten PhCO₂⁻ groups and four (ph)(2-py)CNO⁻ ligands. Bond-valence sum (BVS) calculations[20] give values of 1.9 and 1.3 for O(21) and O(22), respectively, supporting their assignments as oxo [O(21), theoretical value: 2.0] and hydroxo [O(22), theoretical value: 1.0] oxygen atoms. The ten PhCO₂⁻ groups are arranged in three classes: (i) two are monodentate with O(71) and O(71′) being the ligated atoms; (ii) four [those containing O(31)/O(32), O(41)/O(42) and their symmetry-related partners] bridge two Mn ions and are in their familiar *syn,syn*-η^1:η^1:μ_2 binding modes; and (iii) four (the rest) are in the fairly rare η^1:η^2:μ_3 modes, one O bridging two Mn ions and

Table 1. Selected bond lengths (Å) and angles (°) for [Mn(O₂CPh)₂{(ph)(2-py)CNOH}₂]·1.2H₂O (**1·1.2H₂O**)

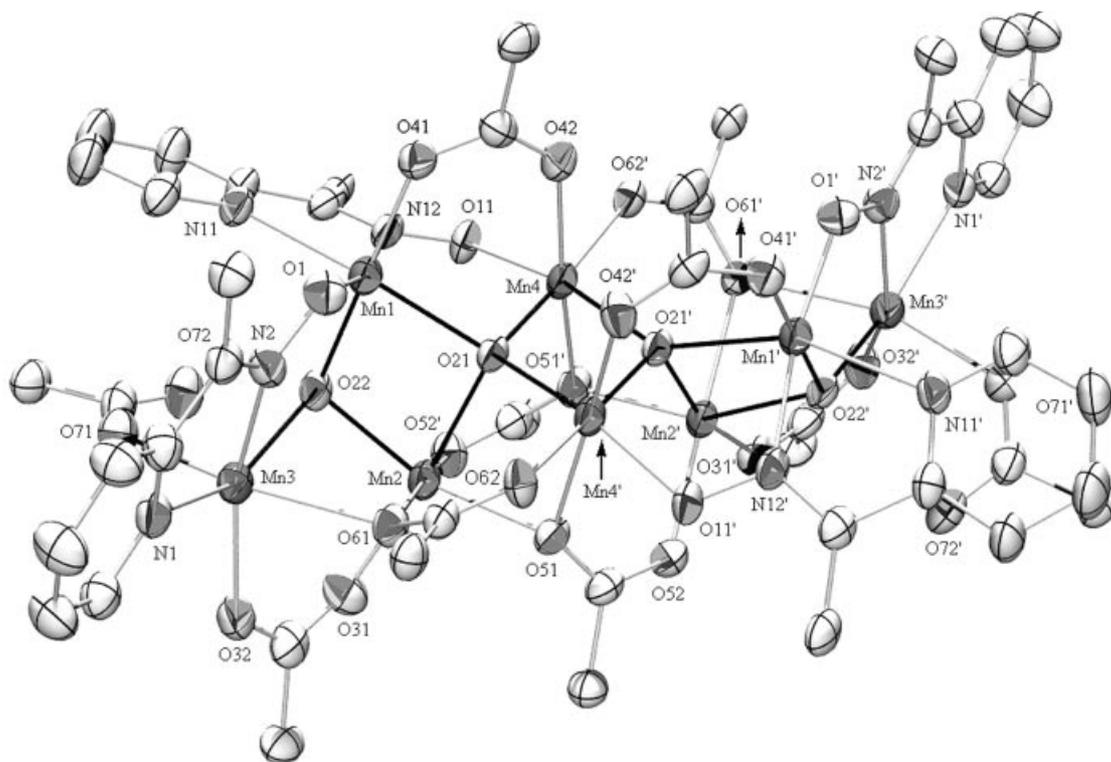|			
Mn−O(21)	2.093(4)	Mn−N(2)	2.255(3)
Mn−O(31)	2.087(3)	Mn−N(12)	2.274(4)
Mn−N(1)	2.319(4)	N(2)−O(1)	1.372(5)
Mn−N(11)	2.281(4)	N(12)−O(11)	1.392(3)
O(21)−Mn−O(31)	90.9(2)	O(31)−Mn−N(12)	96.8(1)
O(21)−Mn−N(1)	171.2(1)	N(1)−Mn−N(11)	94.0(1)
O(21)−Mn−N(11)	87.1(1)	N(1)−Mn−N(2)	70.6(1)
O(21)−Mn−N(2)	100.6(1)	N(1)−Mn−N(12)	91.8(1)
O(21)−Mn−N(12)	96.8(1)	N(11)−Mn−N(2)	97.2(1)
O(31)−Mn−N(1)	89.9(3)	N(11)−Mn−N(12)	70.8(1)
O(31)−Mn−N(11)	167.2(3)	N(2)−Mn−N(12)	158.3(1)
O(31)−Mn−N(2)	95.6(1)		

Figure 3. ORTEP representation of complex **2**; thermal ellipsoids are at the 30% probability level; primed and unprimed atoms are related by a crystallographic inversion centre; only the *ipso* carbon atoms of the phenyl groups of the benzoato and oximato ligands are shown

Table 2. Selected interatomic distances (Å) and angles (°) for $[Mn_8O_2(OH)_2(O_2CPh)_{10}\{(ph)(2\text{-}py)CNO\}_4]\cdot 4CH_2Cl_2$ ($2\cdot 4CH_2Cl_2$)[a]

Mn(1)···Mn(2)	3.270(2)	Mn(2)−O(22)	2.155(5)
Mn(1)···Mn(3)	3.556(2)	Mn(2)−O(31)	2.087(6)
Mn(1)···Mn(4)	3.307(1)	Mn(2)−O(51)	2.133(5)
Mn(2)···Mn(3)	3.368(2)	Mn(2)−O(52′)	2.140(6)
Mn(2)···Mn(4)	3.575(2)	Mn(2)−O(61)	2.308(5)
Mn(3)···Mn(4)	6.062(2)	Mn(3)−O(22)	2.195(5)
Mn(1)···Mn(4′)	3.945(2)	Mn(3)−O(32)	2.067(6)
Mn(2)···Mn(4′)	3.187(2)	Mn(3)−O(61)	2.408(5)
Mn(3)···Mn(4′)	5.367(2)	Mn(3)−O(71)	2.139(6)
Mn(4)···Mn(4′)	2.791(3)	Mn(3)−N(1)	2.269(7)
Mn(1)−O(1)	1.891(6)	Mn(3)−N(2)	2.223(7)
Mn(1)−O(21)	2.235(5)	Mn(4)−O(11)	1.937(5)
Mn(1)−O(22)	1.913(5)	Mn(4)−O(21)	1.872(5)
Mn(1)−O(41)	1.925(5)	Mn(4)−O(21′)	1.898(5)
Mn(1)−N(11)	2.301(6)	Mn(4)−O(42)	2.164(6)
Mn(1)−N(12)	2.050(7)	Mn(4)−O(51′)	2.315(6)
Mn(2)−O(21)	2.274(5)	Mn(4)−O(62′)	1.951(5)

O(1)−Mn(1)−O(21)	107.8(2)	O(32)−Mn(3)−O(61)	80.3(2)
O(1)−Mn(1)−O(22)	95.0(2)	O(32)−Mn(3)−O(71)	97.5(2)
O(1)−Mn(1)−O(41)	83.6(2)	O(32)−Mn(3)−N(1)	98.7(3)
O(1)−Mn(1)−N(11)	94.1(2)	O(32)−Mn(3)−N(2)	156.2(2)
O(1)−Mn(1)−N(12)	166.1(2)	O(61)−Mn(3)−O(71)	161.0(2)
O(21)−Mn(1)−O(22)	83.0(2)	O(61)−Mn(3)−N(1)	107.9(2)
O(21)−Mn(1)−O(41)	96.3(2)	O(61)−Mn(3)−N(2)	82.2(2)
O(21)−Mn(1)−N(11)	156.2(2)	O(71)−Mn(3)−N(1)	91.1(2)
O(21)−Mn(1)−N(12)	85.3(2)	O(71)−Mn(3)−N(2)	104.2(2)
O(22)−Mn(1)−O(41)	178.2(3)	N(1)−Mn(3)−N(2)	71.7(2)
O(22)−Mn(1)−N(11)	85.9(2)	O(11)−Mn(4)−O(21)	93.6(2)
O(22)−Mn(1)−N(12)	91.2(2)	O(11)−Mn(4)−O(21′)	165.2(2)
O(41)−Mn(1)−N(11)	95.3(2)	O(11)−Mn(4)−O(42)	95.2(2)
O(41)−Mn(1)−N(12)	90.4(2)	O(11)−Mn(4)−O(51′)	82.2(2)
N(11)−Mn(1)−N(12)	73.9(2)	O(11)−Mn(4)−O(62′)	86.2(2)
O(21)−Mn(2)−O(22)	77.0(2)	O(21)−Mn(4)−O(21′)	84.4(2)
O(21)−Mn(2)−O(31)	166.8(2)	O(21)−Mn(4)−O(42)	92.4(2)
O(21)−Mn(2)−O(51)	79.5(2)	O(21)−Mn(4)−O(51′)	96.9(2)
O(21)−Mn(2)−O(52′)	100.3(2)	O(21)−Mn(4)−O(62′)	175.5(2)
O(21)−Mn(2)−O(61)	85.8(2)	O(21′)−Mn(4)−O(42)	99.5(2)
O(22)−Mn(2)−O(31)	94.3(2)	O(21′)−Mn(4)−O(51′)	83.5(2)
O(22)−Mn(2)−O(51)	152.2(2)	O(21′)−Mn(4)−O(62′)	97.0(2)
O(22)−Mn(2)−O(52′)	106.4(2)	O(42)−Mn(4)−O(51′)	170.5(2)
O(22)−Mn(2)−O(61)	76.2(2)	O(42)−Mn(4)−O(62′)	82.8(2)
O(31)−Mn(2)−O(51)	105.8(2)	O(51′)−Mn(4′)−O(62′)	87.9(2)
O(31)−Mn(2)−O(52′)	91.7(2)	Mn(1)−O(21)−Mn(2)	93.0(2)
O(31)−Mn(2)−O(61)	82.3(2)	Mn(1)−O(21)−Mn(4)	106.9(2)
O(51)−Mn(2)−O(52′)	92.1(2)	Mn(1)−O(21)−Mn(4′)	145.2(3)
O(51)−Mn(2)−O(61)	87.5(2)	Mn(2)−O(21)−Mn(4)	118.8(2)
O(52′)−Mn(2)−O(61)	173.7(2)	Mn(2)−O(21)−Mn(4′)	99.2(2)
O(22)−Mn(3)−O(32)	109.2(2)	Mn(4)−O(21)−Mn(4′)	95.5(2)
O(22)−Mn(3)−O(61)	73.5(2)	Mn(1)−O(22)−Mn(2)	106.8(2)
O(22)−Mn(3)−O(71)	89.8(2)	Mn(1)−O(22)−Mn(3)	119.7(3)
O(22)−Mn(3)−N(1)	151.7(2)	Mn(2)−O(22)−Mn(3)	101.5(2)
O(22)−Mn(3)−N(2)	80.8(2)		

[a] Primed atoms are related to the unprimed ones by the symmetry transformation −x, y, −z − 1/2.

the other O terminal to a third Mn ion, with the bridging carboxylate O atoms being O(51), O(51′), O(61) and O(61′). The four (ph)(2-py)CNO⁻ ions behave as $\eta^1{:}\eta^1{:}\eta^1{:}\mu_2$ ligands; each ligand chelates one metal ion through its nitrogen atoms forming a five-membered ring and bridges this metal ion with a second one through the terminally ligated, deprotonated O atom [O(1), O(1′),

O(11), O(11′)]. For convenience, the six coordination modes exhibited by the four different ligands of **2** are presented in Figure 4.
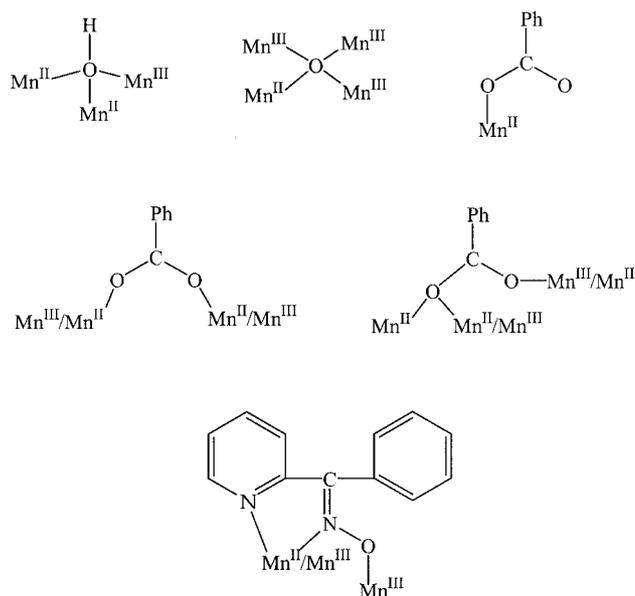

Figure 4. The crystallographically established coordination modes of the hydroxo, oxo, benzoato and phenyl 2-pyridyl ketone oximato ligands present in complex **2**

Mn(1) and Mn(3) are bound to an O_4N_2 set of donor atoms, while Mn(2) and Mn(4) are bound to an O_6 set. Charge considerations require a $4Mn^{II}$, $4Mn^{III}$ oxidation-state description, and Mn(2) and Mn(3) [and their symmetry related Mn(2′) and Mn(3′)] are assigned as the Mn^{II} ions on the basis of: (i) the longer average Mn−O bond lengths at these ions (average 2.190 Å and no individual value shorter than 2.07 Å) compared with those of the other Mn ions (average 2.010 Å), (ii) the clear presence of a Jahn−Teller (JT) axial elongation at Mn(1) and Mn(4) [and their symmetry-related partners], as expected for a high-spin d^4 ion in near-octahedral geometry; the JT elongation axes are O(21)−Mn(1)−N(11) and O(42)−Mn(4)−O(51′), with the axially elongated Mn−O bonds being longer than the equatorial Mn−O bonds by at least 0.21 Å, and (iii) BVS calculations[20] which give values of 3.21, 2.12, 1.75 and 3.20 for Mn(1), Mn(2), Mn(3) and Mn(4), respectively, in good agreement with the above assignments.

The above assignments of the Mn oxidation states reveal that the hydroxo ligand bridges two Mn^{II} and one Mn^{III} ions, while the oxo ligand bridges one Mn^{II} and three Mn^{III} ions (Figure 4). The four $\eta^1{:}\eta^1{:}\mu_2$ $PhCO_2^-$ groups separate further into two subclasses: The groups bearing O(31), O(32) and O(31′), O(32′) each bridge two Mn^{II} ions and those bearing O(41), O(42) and O(41′), O(42′) each bridge two Mn^{III} ions. Similarly, there are two types of $\eta^1{:}\eta^2{:}\mu_3$ $PhCO_2^-$ groups, which all bridge one Mn^{III} and two Mn^{II} ions: the μ_2-O [O(51), O(51′)] of the carboxylate groups bearing O(51), O(52) and O(51′), O(52′) bridges one Mn^{II} and one Mn^{III} ion, whereas the μ_2-O [O(61), O(61′)] of the

groups bearing O(61), O(62) and O(61′), O(62′) bridges two Mn^{II} ions. The four $\eta^1:\eta^1:\eta^1:\mu_2$ (ph)(2-py)CNO⁻ ligands also separate further into two subclasses: The anions bearing N(1), N(2), O(1) and their symmetry-related partners each bridge one Mn^{II} and one Mn^{III} ion, while those bearing N(11), N(12), O(11) and N(11′), N(12′), O(11′) each bridge two Mn^{III} ions; in both cases the deprotonated oximate oxygen atom is terminally ligated to a Mn^{III} ion (Figure 4).

The molecular structure of **2** leads to diverse Mn···Mn distances (Table 2), which depend on the number and nature of the bridges between the two metal centres and on the oxidation state of each Mn atom. The central Mn(4)···Mn(4′) separation is the shortest [2.791(3) Å]; this separation is almost identical to the Mn···Mn distances observed for other polynuclear complexes containing the $[Mn_2^{III}(\mu_4\text{-}O)_2]^{2+}$ subunit.[17] The other two $Mn^{III}···Mn^{III}$ distances are 3.307(2) [Mn(1)···Mn(4)] and 3.945(2) Å [Mn(1)···Mn(4′)]; the shorter Mn···Mn separation corresponds to the pair bridged by one oxo, one $\eta^1:\eta^1:\mu_2$ benzoato and one oximato groups, whereas the larger distance corresponds to that linked by only one oxo group. The shortest $Mn^{II}···Mn^{III}$ distance is Mn(2)···Mn(4′) [3.187(2) Å]; this pair is bridged by one oxo group and the μ_2-O of an $\eta^1:\eta^2:\mu_3$ benzoato group. The μ_2-benzoate oxygen atom O(61) [and O(61′)] does not bridge the two Mn^{II} ions symmetrically, and Mn(2)−O(61) [2.308(5) Å] is noticeably shorter than Mn(3)−O(61) [2.408(5) Å]. The Mn(2,3)−O(22) distances [2.155(5), 2.195(5) Å] are noticeably longer than the Mn(1)−O(22) distance [1.913(5) Å], consistent with the lower oxidation state in the former. Similarly, Mn(2,3)-carboxylate distances (average 2.190 Å) are longer than Mn(1,4)-carboxylate distances (average 2.090 Å). It is interesting that the $\mu_4\text{-}O^{2-}$ ions [O(21), O(21′)] bridge the Mn^{III} ions asymmetrically. Thus, Mn(4)−O(21) and Mn(4′)−O(21) are 1.872(5) and 1.898(5) Å, respectively, whereas Mn(1)−O(21) is much longer at 2.235(5) Å. This is the result of O(21) lying on the JT elongation axis of Mn(1); $Mn^{III}−O^{2-}$ distances greater than 2.2 Å are extremely rare.[21] This JT-elongated Mn(1)−O(21) bond contributes to the relatively long Mn(1)···Mn(4′) distance [3.945(2) Å].

The uncoordinated O atoms of the monodentate $PhCO_2^-$ groups [O(72) and O(72′)] are hydrogen-bonded to the μ_3-OH⁻ ligands, with the O(72)···O(22) distance being 2.610 Å.

The novel Mn_8 topology in **2** can be described in a number of ways, but the following three are particularly useful. As is emphasised in Figure 5, the $[Mn_8O_2(OH)_2]^{14+}$ core can be conveniently described as two $\{Mn_2^{II}Mn_2^{III}(\mu_3\text{-}O)(\mu_3\text{-}OH)\}^{7+}$ units [atoms Mn(1)−Mn(4) and their symmetry-related partners] becoming linked through the μ_3-O^{2-} in each unit converting to a μ_4 mode and thus providing the two "inter-fragment' bonds Mn(4)−O(21′) and Mn(4′)−O(21). The four metal ions in each unit are nearly coplanar with the torsion angle Mn(1)−Mn(2)−Mn(3)−Mn(4) being 9.4°. Although tetranuclear complexes containing the $[Mn_4(\mu_3\text{-}O)_2]$ core, where the metals are arranged in either planar or nonplanar ("butterfly") fashion and the metal oxidation levels are $Mn_2^{II}Mn_2^{III}$,[22] $Mn^{II}Mn_3^{III}$[23] or Mn^{III},[15,22] have been reported, the $\{Mn_2^{II}Mn_2^{III}(\mu_3\text{-}O)(\mu_3\text{-}OH)\}^{7+}$ unit present in **2** has not been observed either in a discrete tetranuclear complex or encountered as a recognizable sub-fragment of higher nuclearity Mn clusters. A second way of describing the core emphasises its "central" $\{Mn_2^{II}Mn_4^{III}(\mu_4\text{-}O)_2\}^{12+}$ subunit, which is the currently unknown (in either a discrete hexanuclear complex or in a higher nuclearity cluster) oxidized version of the familiar[17] $[Mn_4^{II}Mn_2^{III}(\mu_4\text{-}O)_2]^{10+}$ core; extension of the former at each end with an additional Mn^{II} ion through the μ_3-OH⁻ gives the core of **2**. In view of the magnetochemical discussion presented below (vide infra), it is of interest and beneficial to consider a third, alternate description of the core of complex **2** which emphasises its structural relationship to a well-known smaller nuclearity Mn/O unit. The molecule can be described as consisting of a central, butterfly-like[15,22] $[Mn_4^{III}(\mu_3\text{-}O)_2]^{8+}$ subunit [atoms Mn(1), Mn(1′), Mn(4), Mn(4′), O(21), O(21′); see Figure 5]. The $[Mn_8(\mu_4\text{-}O)_2(\mu_3\text{-}OH)_2]^{14+}$ core of **2** is then completed by the attachment of two additional $[Mn_2^{II,II}(\mu_2\text{-}OH)]^{3+}$ subunits to the butterfly-like central sub-core via the inter-fragment bonds Mn(1)−O(22), Mn(2)−O(21) and their symmetry equivalents. As a result, each OH⁻ ligand becomes μ_3, forming a bond with a "wing-tip" Mn^{III} ion [Mn(1), Mn(1′)], and each O^{2-} ligand is converted to μ_4, forming a bond with one of the Mn^{II} ions [Mn(2), Mn(2′)].

Complex **2** joins a very small family of Mn clusters of nuclearity eight, which currently comprise the metal oxi-
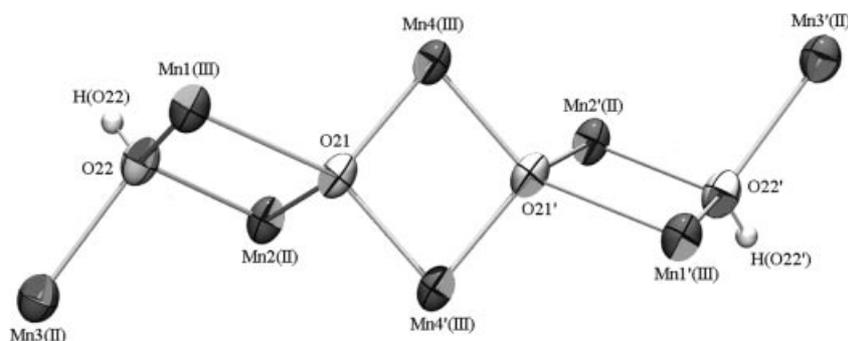

Figure 5. ORTEP representation of the $[Mn_4^{II}Mn_4^{III}(\mu_4\text{-}O)_2(\mu_3\text{-}OH)_2]^{14+}$ core of **2**

dation states Mn_8^{II},[24] $Mn_6^{II}Mn_2^{III}$,[6a,25] $Mn_2^{II}Mn_6^{III}$,[15,26] Mn_8^{III} [18a,27] and $Mn_2^{III}Mn_6^{IV}$,[28] and thus becomes the first member of the $Mn_4^{II}Mn_4^{III}$ subfamily. Since most of these were reported only recently, we felt it timely to collect the octanuclear $Mn^{II/III}$, Mn^{III} and $Mn^{III/IV}$ clusters in Table 3, together with their cores for convenient comparison; we have not included the Mn_8^{II} complexes. The $[Mn_4^{II}\text{-}Mn_4^{III}(\mu_4\text{-O})_2(\mu_3\text{-OH})_2]^{14+}$ core of **2** bears some similarity to the $[Mn_2^{II}Mn_6^{III}(\mu_3\text{-O})_2(\mu_4\text{-O})_2]^{14+}$ core present[15] in the anion $[Mn_8O_4(O_2CPh)_{12}(Et_2mal)_2(H_2O)_2]^{2-}$, where Et_2mal is the dianion of 2,2-diethylmalonic acid; the former can be thought of as being derived from the latter by reduction/protonation steps. Complex **2** is also one of the rare examples of polynuclear Mn complexes that contain oxo and hydroxo bridges simultaneously,[29] other such complexes being $[Mn_8O_4(OH)_2(O_2CMe)_{12}(DMHP)_2(py)_2]$ (DMHP = 2,6-dimethyl-6-hydroxypyrimidine; py = pyridine),[26] $[Mn_4O_5(OH)(tame)_4](CF_3SO_3)_5$ [tame= 1,1,1-tris(aminomethyl)ethane],[30] $[Mn_4O_5(OH)(tacn)_4](ClO_4)_5$ (tacn = 1,4,7-triazacyclononane)[30] and $[Mn_{10}O_4(OH)_2(O_2CMe)_8(hmp)_8](ClO_4)_4$ [hmp = the anion of 2-(hydroxymethyl)pyridine].[16]

The Mn_8 nuclearity of **2** can be put into context by noting that the largest molecular Mn cluster currently known is $[Mn_{30}O_{24}(OH)_8(O_2CCH_2But)_{32}(H_2O)_2(MeNO_2)_4]$,[31a] followed by $[Mn_{26}O_{16}(OH)_{10}(OMe)_6F_{10}(bta)_2(btaH)_2(MeOH)_{13}(H_2O)]$, where btaH is benzotriazole;[31b] these two clusters are also mixed oxo/hydroxo species.

$[Mn_3(O_2CPh)_6\{(ph)(2\text{-py})CO\}_2]$ (3)

A partially labelled plot of the trinuclear complex **3** is shown in Figure 6. Selected interatomic distances and angles are listed in Table 4. The complex crystallises in the monoclinic space group $P2_1/a$. The central metal ion, Mn(2), which is located on a crystallographic inversion centre, is coordinated octahedrally by six oxygen atoms belonging to six different benzoates. Thus, the trinuclear molecule adopts a linear structure, with one $\eta^1:\eta^2:\mu_2$ and two *syn,-syn*-$\eta^1:\eta^1:\mu_2$ carboxylate groups spanning each pair of Mn^{II}. The termini of the $\{Mn(O_2CPh)_3Mn(O_2CPh)_3Mn\}$ unit are capped by bidentate chelating (ph)(2-py)CO ligands, resulting in six-coordination at these sites.

Table 3. Formulae, cores and core description for structurally characterised octanuclear $Mn^{II/III}$, Mn^{III} and $Mn^{III/IV}$ clusters

Complex[a]	Core	Core description	Ref.
$[Mn_8O_2(O_2CCH_2tBu)_{14}(ButCH_2CO_2H)_4]$	$[Mn_6^{II}Mn_2^{III}(\mu_4\text{-O})_2(\mu_2\text{-O})_8]^{10+[b]}$	extension of the $[Mn_4^{II}Mn_2^{III}(\mu_4\text{-O})_2]^{10+}$ core at one end with two additional Mn^{II} ions	[25]
$[Mn_8O_2(O_2CEt)_8(py)_4(L)_2]^{2+}$	$[Mn_6^{II}Mn_2^{III}(\mu_4\text{-O})_2(\mu_3\text{-O})_4(\mu_2\text{-O})_4]^{6+[c]}$	two distorted cubanes edge-linked together at two Mn−O edges	[6a]
$[Mn_8O_2(OH)_2(O_2CPh)_{10}\{(ph)(2\text{-py})CNO\}_4]$	$[Mn_4^{II}Mn_4^{III}(\mu_4\text{-O})_2(\mu_3\text{-OH})_2]^{14+}$	two $\{Mn_2^{II}Mn_2^{III}(\mu_3\text{-O})(\mu_3\text{-OH})\}^{7+}$ units linked *via* the O^{2-} in each unit	this work
$[Mn_8O_4(OH)_2(O_2CMe)_{12}(DMHP)_2(py)_2]$	$[Mn_2^{II}Mn_6^{III}(\mu_3\text{-O})_4(\mu_2\text{-OH})_2]^{12+}$	two $[Mn^{II}Mn_3^{III}(\mu_3\text{-O})_2]^{7+}$ "butterfly" units linked by the two $\mu_2\text{-OH}^-$ ligands	[26]
$[Mn_8O_4(O_2CPh)_{12}(Et_2mal)_2(H_2O)_2]^{2-}$	$[Mn_2^{II}Mn_6^{III}(\mu_4\text{-O})_2(\mu_3\text{-O})_2]^{14+}$	two $[Mn^{II}Mn_3^{III}(\mu_3\text{-O})_2]^{7+}$ "butterfly" units linked by one O^{2-} in each unit	[15]
$[Mn_8O_4(O_2CMe)_{12}(pic)_4]$	$[Mn_4^{III}(\mu_3\text{-O})_2]_2^{8+}$	two $[Mn_4^{III}(\mu_3\text{-O})_2]^{8+}$ units linked through two picolinates bridges	[27a]
$[Mn_8O_6Cl_6(O_2CPh)_7(H_2O)_2]^-$	$[Mn_8^{III}(\mu_4\text{-O})_2(\mu_3\text{-O})_4(\mu_2\text{-Cl})_2(\mu_3\text{-Cl})(\mu_4\text{-Cl})]^{8+}$	two $[Mn_4^{III}(\mu_3\text{-O})_2]^{8+}$ "butterfly" units fused by sharing one "body" Mn; an eighth Mn^{III} ion is connected to the resultant $\{Mn_7O_7\}^{7+}$ unit by two additional bridging O^{2-} ions	[18a]
$[Mn_8O_4(piv)_{10}(thme)_2(py)_2]$	$[Mn_8^{III}(\mu_3\text{-O})_4]^{16+}$	six edge-sharing triangles or three edge-sharing "butterfly" units (ladder-like unit)	[27b]
$[Mn_8O_4(O_2CPh)_{12}(dbm)_4(bpe)_2]$	$[Mn_4^{III}(\mu_3\text{-O})_2]_2^{8+}$	two "butterfly" $[Mn_4^{III}(\mu_3\text{-O})_2]^{8+}$ units with the two bpe ligands attached *syn* about the central $[Mn_2O_2]$ rhomboids	[27c]
$[Mn_8O_4(O_2CEt)_{14}(py)_4(L')_2]^{2+}$	$[Mn_4^{III}(\mu_3\text{-O})_2]_2^{8+}$	two butterfly-like cores arranged face-to-face and bridged by two bis-bidentate L ligands	[27d]
$[Mn_8O_{10}(O_2CMe)_6(bpy)_2(H_2O)_2]^{4+}$	$[Mn_2^{III}Mn_6^{IV}(\mu_2\text{-O})_8(\mu_3\text{-O})_2]^{10+}$	five $[Mn_2O_2]$ rhombs linked and fused to give a core with a serpentine topology	[28]

[a] Counterions and solvate molecules omitted; bpe = *trans*-1,2-bis(4-pyridyl)ethene; bpy = 2,2′-bipyridine; dbm = the anion of dibenzoylmethane; DMHP = 2,6-dimethyl-6-hydroxypyrimidine; Et_2mal = the dianion of 2,2-diethylmalonic acid; L = the dianion of (6-hydroxymethylpyridin-2-yl)-(6-hydroxymethylpyridin-2-yl methoxymethanol); L′ = 1,2-bis(5-methyl-2,2′-bipyridyl-5-yl)ethane; pic = the picolinate anion; piv = the pivalate anion; py = pyridine. [b] The μ_2-O atoms belong to carboxylates. [c] The μ_3-O atoms belong to the L^{2-} ligands, while the μ_2-O atoms are from $EtCO_2^-$ ligands.
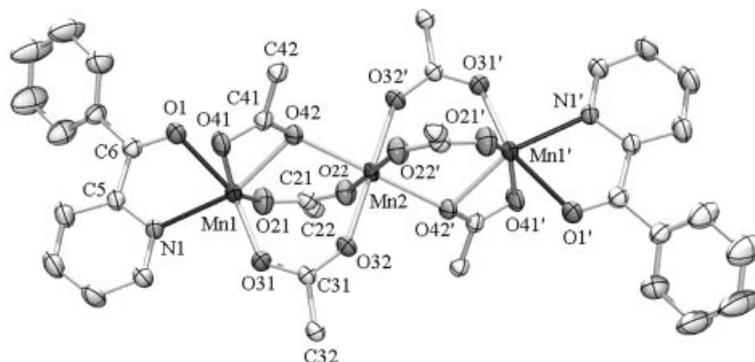
Figure 6. ORTEP drawing showing 30% probability ellipsoids and labelling scheme for complex **3**; primed and unprimed atoms are related by a crystallographic inversion centre; only the *ipso* carbon atoms of the phenyl rings of the benzoato ligands are shown

Table 4. Selected interatomic distances (Å) and angles (°) for $[Mn_3(O_2CPh)_6\{(ph)(2\text{-py})CO\}_2]$ (**3**)[a]

Mn(1)···Mn(2)	3.603(5)	Mn(2)−O(32)	2.136(3)
Mn(1)···Mn(1′)	7.205(5)	Mn(2)−O(42)	2.240(3)
Mn(1)−O(1)	2.339(4)	C(6)−O(1)	1.224(5)
Mn(1)−N(1)	2.256(4)	C(21)−O(21)	1.258(5)
Mn(1)−O(21)	2.058(4)	C(21)−O(22)	1.239(5)
Mn(1)−O(31)	2.086(3)	C(31)−O(31)	1.249(5)
Mn(1)−O(41)	2.249(4)	C(31)−O(32)	1.247(5)
Mn(1)−O(42)	2.261(3)	C(41)−O(41)	1.247(5)
Mn(2)−O(22)	2.156(3)	C(41)−O(42)	1.275(5)
O(1)−Mn(1)−N(1)	70.4(1)	O(22)−Mn(2)−O(22′)	180.0(1)
O(1)−Mn(1)−O(21)	88.1(1)	O(22)−Mn(2)−O(32)	91.3(1)
O(1)−Mn(1)−O(31)	159.7(1)	O(22)−Mn(2)−O(32′)	88.7(1)
O(1)−Mn(1)−O(41)	81.3(1)	O(22)−Mn(2)−O(42)	89.6(1)
O(1)−Mn(1)−O(42)	96.6(1)	O(22)−Mn(2)−O(42′)	90.5(1)
N(1)−Mn(1)−O(21)	103.1(2)	O(22′)−Mn(2)−O(32)	88.7(1)
N(1)−Mn(1)−O(31)	89.8(1)	O(22′)−Mn(2)−O(32′)	91.3(1)
N(1)−Mn(1)−O(41)	99.5(1)	O(22′)−Mn(2)−O(42)	90.5(1)
N(1)−Mn(1)−O(42)	156.2(1)	O(22′)−Mn(2)−O(42′)	89.6(1)
O(21)−Mn(1)−O(31)	101.2(2)	O(32)−Mn(2)−O(32′)	180.0(1)
O(21)−Mn(1)−O(41)	150.1(1)	O(32)−Mn(2)−O(42)	93.0(1)
O(21)−Mn(1)−O(42)	96.2(1)	O(32)−Mn(2)−O(42′)	87.0(1)
O(31)−Mn(1)−O(41)	98.2(1)	O(32′)−Mn(2)−O(42)	87.0(1)
O(31)−Mn(1)−O(42)	100.3(1)	O(32′)−Mn(2)−O(42′)	93.0(1)
O(41)−Mn(1)−O(42)	57.9(1)	O(42)−Mn(2)−O(42′)	180.0(1)
C(21)−O(21)−Mn(1)	130.6(3)	C(21)−O(22)−Mn(2)	142.0(3)
C(31)−O(31)−Mn(1)	130.9(3)	C(31)−O(32)−Mn(2)	142.3(3)
C(41)−O(41)−Mn(1)	91.6(3)	C(41)−O(42)−Mn(1)	90.3(3)
O(21)−C(21)−O(22)	125.4(5)	C(41)−O(42)−Mn(2)	140.2(3)
C(22)−C(21)−O(21)	116.2(4)	O(41)−C(41)−O(42)	119.9(4)
C(22)−C(21)−O(22)	118.4(4)	C(42)−C(41)−O(41)	119.9(4)
O(31)−C(31)−O(32)	124.7(4)	C(42)−C(41)−O(42)	120.2(4)
C(32)−C(31)−O(31)	117.7(4)	Mn(1)−O(42)−Mn(2)	106.3(4)
C(32)−C(31)−O(32)	117.6(4)		

[a] Primed atoms are related to the unprimed ones by the symmetry transformation −x, −y + 1, −z.

The Mn(1) polyhedron is significantly distorted. The main distortions arise from the five-membered chelating ring with a narrow O(1)−Mn(1)−N(1) bond angle [70.4(1)°] and an acute O(41)−Mn(1)−O(42) angle [57.9(1)°]. The Mn−N and Mn−O bond lengths agree well with values expected for high-spin Mn[II].[13] The Mn(2)−O

bond lengths are in the narrow 2.136(3)−2.240(3) Å range, with the Mn(2)−O(42) distance longer, as expected. The coordination of the bridging benzoate oxygen, O(42) [and O(42′)], is somewhat pyramidal [$\Sigma°O(42) = 336.8°$].

Complex **3** joins a small family[32−34] of trinuclear Mn[II] carboxylate complexes containing the $[Mn_3(\eta^1:\eta^1:\mu_2\text{-}O_2CR)_4(\eta^1:\eta^2:\mu_2\text{-}O_2CR)_2]^0$ core. The members of this family are listed in Table 5. This structural motif was also confirmed[35] for complexes $[Mn_3(O_2CPh\text{-}3\text{-}Cl)_6(bpy)_2]$ and $[Mn_3(O_2CPh\text{-}3\text{-}Cl)_6(Me_2\text{-}bpy)_2]$ (Me$_2$-bpy = 4,4′-dimethyl-2,2′-bipyridine) by analysis of the XANES and EXAFS spectra at the Mn K-edge; since only average distances could be derived, these two complexes are not included in Table 5. Some of the listed complexes have been important in the establishment of the "carboxylate shift" model.[34] Of the various types of metal-carboxylate binding modes, monodentate(monoatomic) bridging between metal centres offers unique flexibility. Analysis[34] of the structural characteristics of discrete compounds containing monodentate (monoatomic) bridging carboxylates shows that they can be arranged into three classes, depending upon the strength of the interaction of the non-bridging, or dangling (O$_d$), oxygen atom [O(42) in complex **3**] with one of the bridged metal ions [Mn(1) in **3**]. The application of this analysis to trinuclear Mn[II] carboxylate complexes is demonstrated in Figure 7 and Table 5. The monodentate bridging mode is postulated to be an important intermediate between the other, more common, carboxylate attachment modes, based on observed variations of the geometry for monodentate bridges in structurally characterised complexes. The movement from monodentate to these other binding modes has been termed the "carboxylate shift";[34] such a shift could be kinetically important in carboxylate-containing metalloproteins.

Complex **3** is characterised by a small *D* value, *B* > *D*, a rather large Mn···Mn distance, a small difference between C−O$_d$ and C−O$_b$ (indicating significant delocalisation of the double bond), a large tilt (α-β) of the $\eta^1:\eta^2:\mu_2$ carboxylate toward Mn(1) and a significant distortion of the coordination geometry of Mn(1). Thus, complex **3** has a

Table 5. Pertinent structural[a] and magnetic properties for trinuclear manganese(II) complexes containing the [Mn₃(η^1:η^1:μ_2-O₂CR)₄(η^1:η^2:μ_2-O₂CR)₂]⁰ core; bpy = 2,2′-bipyridine; L = 2,2′-bis(1-methylimidazolyl)phenylmethoxymethane; phen = 1,10-phenanthroline; pybim = 2-(2-pyridyl)benzimidazole

Complex	B (Å)	D (Å)	A (Å)	Mn···Mn (Å)	$C-O_b$ (Å)	$C-O_d$ (Å)	θ (°)	β (°)	α (°)	J (cm⁻¹)	S	Ref.
[Mn₃(O₂CMe)₆(pybim)₂]	2.132	2.283	2.235	3.558	[b]	[b]	109.1	[b]	[b]	−1.9	5/2	[32a]
[Mn₃(O₂CMe)₆(bpy)₂]	2.155	2.605	2.200	3.614	1.276	1.228	112.2	[b]	[b]	−4.4	5/2	[32b]
anti-[Mn₃(O₂CMe)₆L₂] (A)[c]	2.172	2.488	2.205	3.635	1.28(1)	1.22(1)	112.3	98.9	136.1			[32c]
anti-[Mn₃(O₂CMe)₆L₂] (B)[c]	2.263[d]	2.325[d]	2.236[d]	3.708[d]	1.272[d]	1.250[d]	111.0[d]	92.0[d]	131.1[d]	−2.8[e]		[32c]
syn-[Mn₃(O₂CMe)₆L₂][c]	2.190[f]	2.580[f]	2.191[f]	3.465[f]	1.27(1)[f]	1.25(1)[f]	104.6[f]	102.0[f]	143.4[f]			[32c]
[Mn₃(O₂CMe)₆(phen)₂][g]	2.285	2.425	2.133	3.387	1.263	1.224	100.1	99.9	144.9	[h]	[h]	[32c]
[Mn₃(O₂CPh)₆(bpy)₂]	2.285	2.274	2.239	3.588	1.284	1.257	104.9	90.5	135.0	[h]	[h]	[32d]
[Mn₃(O₂CPh)₆{(ph)(2-py)CO}₂]	2.261	2.249	2.240	3.603	1.275	1.247	106.3	90.3	140.2	−2.7	5/2	this work
(Et₄N)₂[Mn₃(O₂CMe)₈]	2.17	2.14	2.11	3.569	[b]	[b]	[b]	[b]	[b]	−5.6	5/2	[32e]

[a] See Figure 7 for the definition of the structural parameters given in this table. [b] Not reported. [c] Three isomers of [Mn₃(O₂CMe)₆L₂] have been crystallised and structurally characterised; they are designated *anti* and *syn* based on the disposition of the L imidazole groups with respect to the best plane passing through the three metal ions and the two monodentate acetate oxygen bridges. The A designation indicates the *anti* isomer where the central metal is located on a crystallographic inversion centre; no such inversion centre exists in the B form. [d] Average value for one of the two crystallographically independent trinuclear molecules present in the unit cell. [e] Variable-temperature magnetic-susceptibility data are available for a bulk sample of [Mn₃(O₂CMe)₆L₂] possibly containing all three isomers. [f] Average value. [g] The single-crystal structure of this complex was also reported by Miyamae and co-workers;[32f] the quoted bond lengths and angles do no differ much from those reported by Lippard and co-workers. [h] Variable-temperature magnetic susceptibility data are not available.
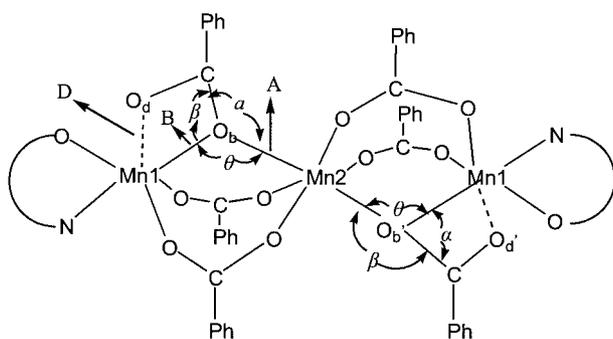

Figure 7. The schematic structure of complex **3** showing the dangling (O_d) and the bridging (O_b) oxygen atoms of the η^1:η^2:μ_2 carboxylate groups, and defining the geometry of monoatomic carboxylate-bridged polymetallic centres in relation to the "carboxylate shift" mechanism proposed by Lippard;[32c,34] the values of the relevant structural parameters for **3** and other trinuclear complexes containing the [Mn₃(η^1:η^1:μ_2-O₂CR)₄(η^1:η^2:μ_2-O₂CR)₂]⁰ core are listed in Table 5.

strong interaction between Mn(1) and O_d, i.e. O(42), and can be placed in class III in Lippard's classification scheme.[34]

IR Spectra

The presence of both neutral oxime and solvate H₂O molecules in **1**·1.2H₂O is manifested by a broad IR band of medium intensity at 3434 cm⁻¹, assigned to $\nu(OH)_{oxime}$ [13]/$\nu(OH)_{water}$.[36] The IR spectrum of **2** exhibits a medium band at 3438 cm⁻¹ assignable[37] to $\nu(OH)_{OH^-}$; the broadness and relatively low frequency of this band are both indicative of strong hydrogen bonding.

The $\nu(C=O)$ mode is found at a lower wavenumber (1648 cm⁻¹) in the spectrum of **3** than for free (ph)(2-py)CO (1668 cm⁻¹); this shift is consistent with ketone-O coordination.[38]

Several bands appear in the 1610−1390 cm⁻¹ range in the spectra of **1**−**3**. Contributions from the $PhCO_2^-$ $\nu_{as}(CO_2)$ and $\nu_s(CO_2)$ modes would be expected in this region, but overlap with the stretching vibrations of the aromatic rings and $\nu(C=N)_{oxime}$ (in **1** and **2**) renders assignments tentative and application of the spectroscopic criterion of Deacon and Phillips[39a] difficult. In all spectra, the very strong band at 1404−1400 cm⁻¹ should have a high $\nu_s(CO_2)$ character.[13,39b]

A medium-intensity band at 606 cm⁻¹ is present in the spectrum of **2**. This band is absent from the spectra of **1**·1.2H₂O and can be tentatively assigned to a vibration involving a $Mn^{III}-O^{2-}$ stretch.[40]

Magnetic Properties

Complex 2

Solid-state variable-temperature dc magnetic-susceptibility measurements were performed on a microcrystalline sample of **2** in a 0.1 T field in the range 2.0−300 K. The $\chi_M T$ vs. T and χ_M vs. T plots are shown in Figure 8. The value of $\chi_M T$ gradually decreases from 25.2 cm³·mol⁻¹·K at room temperature to 0.82 cm³·mol⁻¹·K at 2.0 K. The value of $\chi_M T$ at room temperature is lower than that expected for a cluster of 4Mn^{II} and 4Mn^{III} non-interacting ions (29.5 cm³·mol⁻¹·K for $g = 2$). A well-defined maximum of χ_M appears at 16 K. The $\chi_M T$ vs. T plot extrapolates to $\chi_M T \approx 0$ as the temperature approaches zero, indicating an $S = 0$ ground state. The intense drop of $\chi_M T$ with decreasing temperature reflects the presence of strong antiferromagnetic interactions within the cluster.

Complex **2** contains 4Mn^{II} and 4Mn^{III} centres, with total spin values ranging from 0 to 18. Owing to the size and low symmetry of the molecule, it is not possible to apply the Kambe method[41] or otherwise evaluate the individual
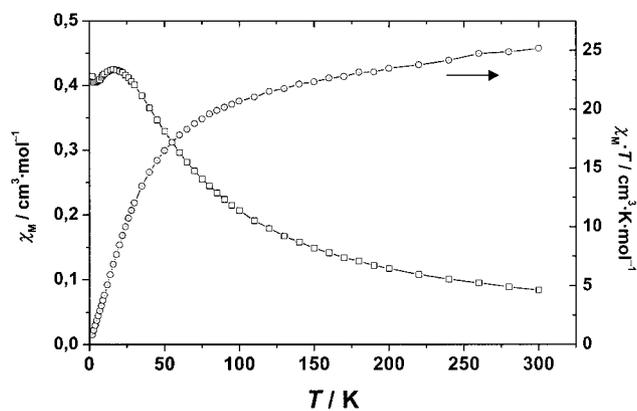
Figure 8. $\chi_M T$ vs. T and χ_M vs. T plots for complex **2**; the solid lines are guides for the eye

pairwise Mn_2 exchange interactions. Magnetisation data were collected in the magnetic field and temperature ranges $1-50$ KG and $2.0-4.0$ K, respectively. These measurements are poorly indicative, because they reveal a continuous increase of M with a change in the slope at 20 KG, up to an $M/N\beta$ value of 5.2 at 50 KG, far from saturation, indicating that several spin-states different from zero are very close to the ground state.

For the present $Mn_4^{II}Mn_4^{III}$ complex **2** it is important to rationalize the apparent $S = 0$. As indicated above, complex **2** can be described as arising from the linkage of the central $[Mn_4^{III}(\mu_3\text{-}O)_2]^{8+}$ subunit with two $[Mn_2^{II,II}(\mu_2\text{-}OH)]^{3+}$ subunits. Since $Mn^{II}\cdots Mn^{II}$ and $Mn^{II}\cdots Mn^{III}$ exchange interactions are typically weak and antiferromagnetic,[6a] the apparent $S = 0$ ground state of **2** can be rationalised taking as a starting point the well-established magnetic behaviour of the central, butterfly-like $[Mn_4^{III}(\mu_3\text{-}O)_2]^{8+}$ sub-core.

Table 6 conveniently summarises all previous magnetochemically characterised, *discrete* $[Mn_4^{III}(\mu_3\text{-}O)_2]^{8+}$ complexes.[22,42] There are two main exchange parameters: a body-body interaction parameter, J_{bb}, and a wing-tip-body parameter, J_{wb}. It has been found in all studied complexes that both types of interaction are antiferromagnetic and that $|J_{bb}|$ is appreciably larger than $|J_{wb}|$. In the format[42d] (S, S_{bb}, S_{ww}), the ground state of most complexes is (3, 1, 4). Even though both types of pairwise exchange interactions are antiferromagnetic, the ground state of these complexes has six unpaired electrons ($S = 3$). Because the J_{bb} interaction is greater than J_{wb} ($J_{bb}/J_{wb} = 3.0-5.0$), the

spins on the two Mn_b ions have a greater tendency to pair up. Each Mn_w ion interacts with both the Mn_b ions and would align its spin antiparallel to both if possible, but it cannot do so. The net result is that the spin alignments of the Mn_w ions are frustrated. Overall, the unpaired electrons on the Mn_b ions are essentially paired up (actually the resultant spin vector S_{bb} is 1, not 0), and this leaves the unpaired electrons on the Mn_w ions. The S_{bb} resultant spin then couples with the $S_{ww} = 4$ to give the resultant $S = 3$ ground state of the complete molecule.[18a] The (3, 1, 4) ground state can be depicted diagrammatically as shown in **I** of Figure 9. In one complex, namely $[Mn_4O_2(O_2CEt)_7(bpya)_2](ClO_4)$ [bpya = bis(2-pyridyl)-amine],[42c] the J_{bb}/J_{wb} ratio is large (7.8) and there is also a very small J_{ww} interaction (-0.8 cm^{-1}); in this case, the spins of the Mn_b ions are fully antiparallel-aligned, i.e. $S_{bb} = 0$, and the ground state is then determined by the interaction of the Mn_w ions via the J_{ww} exchange, giving an $S = 0$ ground state since J_{ww} is antiferromagnetic (**II** in Figure 9). In effect, this (0, 0, 0) ground state can be described as the result of a weak, long-distance J_{ww} interaction between the wing-tip Mn^{III} ions through a strongly coupled, diamagnetic ($S_{bb} = 0$) central unit.[42c] In complex $[Mn_4O_2(O_2CPh)_6(dpm)_2]$ (dpm is the anion of dipivaloylmethane),[42d] the J_{bb}/J_{wb} ratio is much larger (ca. 70) and J_{ww} is negligible, i.e. $J_{ww} = 0$; the (n, 0, n) ground state is best described as fivefold degenerate (**III** in Figure 9). An alternative and completely equivalent description is to suggest that the ground state is composed of two non-interacting independent Mn^{III} ions.[42d]

The core of complex **2** (Figure 5) is more complicated than the $[Mn_4^{III}(\mu_3\text{-}O)_2]^{8+}$ core present in the *discrete* tetranuclear manganese(III) clusters mentioned above. However, the magnetic study of the latter has shown two important features. First, the J_{bb} coupling constant is always negative and relatively strong, and second, ground states with $S \neq 0$ are strongly dependent on the presence of competitive interactions in the coupling scheme. Complex **2** has two possible ligand types which may be involved in competitive interactions; these are the $\mu_4\text{-}O^{2-}$ and the $\mu_3\text{-}OH^-$ ligands. Spin frustration derived from competitive interactions involving the $\mu_4\text{-}O^{2-}$ ligand can be excluded because Mn(1) and Mn(2) are asymmetrically linked to the central Mn(4) and Mn(4') ions, breaking the possible spin frustration. In fact, due to the fact that the oxo group O(21) lies on the JT

Table 6. Exchange interaction constants and ground state spin for the previous magnetochemically characterised, discrete $[Mn_4^{III}(\mu_3\text{-}O)_2]^{8+}$ complexes; bpy = 2,2'-bipyridine; bpya = bis(2-pyridyl)amine; dbm = the anion of dibenzoylmethane; pic = the picolinate anion; py = pyridine

Complex[a]	J_{wb} (cm^{-1})	J_{bb} (cm^{-1})	J_{bb}/J_{wb}	(S, S_{bb}, S_{ww})	Ref.
$[Mn_4O_2(O_2CMe)_7(bpy)_2]^+$	-7.8	-23.5	3.0	(3, 1, 4)	[22]
$[Mn_4O_2(O_2CMe)_7(pic)_2]^-$	-5.3	-24.6	4.6	(3, 1, 4)	[42a]
$[Mn_4O_2(O_2CMe)_6(py)_2(dbm)_2]$	-5.0	-24.9	5.0	(3, 1, 4)	[42b]
$[Mn_4O_2(O_2CEt)_7(bpya)_2]^+$	-3.3	-25.7	7.8	(0, 0, 0)	[42c]
$[Mn_4O_2(O_2CPh)_6(dpm)_2]$	-0.4	-27.5	68.8	(n, 0, n)	[42d]

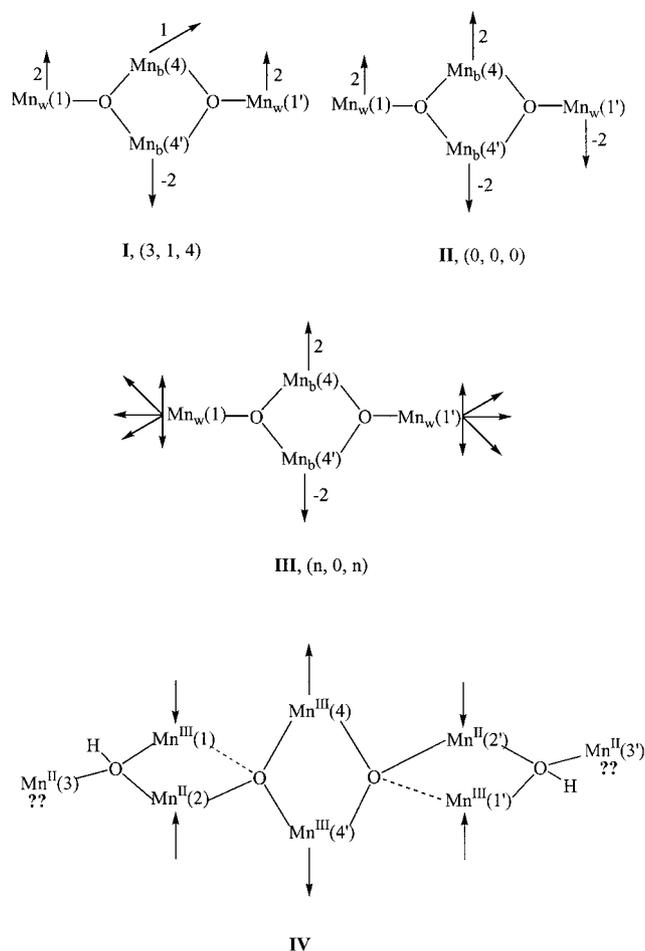[a] Counterions and solvate molecules omitted.

Figure 9. The spin ground states established for *discrete* tetranuclear manganese(III) clusters containing the butterfly-like [Mn$_4^{III}$(μ_3-O)$_2$]$^{8+}$ core (**I**, **II**, **III**) and a tentative coupling scheme for complex **2** (**IV**); the numbering scheme (in parentheses) for the Mn^{III} ions in the tetranuclear complexes is the same as that used for the central, Mn^{III}-containing subunit of complex **2** (see Figure 5), while the subscripts b and w denote body and wing-tip Mn^{III} ions, respectively; in **IV** the oxidation states of the Mn atoms are also denoted by superscripts

elongation axis of Mn(1), the interaction of Mn(1) with Mn(4′) should be very weak and clearly weaker than the interaction between Mn(1) and Mn(4) through the oximato/carboxylate bridges; an antiparallel alignment of the Mn(1) spin vector with respect to Mn(4) should be expected. Mn(2) is also asymmetrically linked to Mn(4) and Mn(4′) [for example, the Mn(2)−O(21)−Mn(4) bond angle is 118.8°, whereas the Mn(2)−O(21)−Mn(4′) one is 99.2°] and therefore different antiferromagnetic coupling with each of these Mn^{III} centres should be expected. These latter competitive interactions, combined with the antiferromagnetic coupling expected through the double oxo-hydroxo bridge within the Mn(2)···Mn(1) pair, make an antiparallel alignment of the Mn(2) spin vector with respect to Mn(1) reasonable. At this point, a reasonable coupling scheme for **2** can be as shown in **IV** of Figure 9, on the basis of the strong antiferromagnetic coupling within the Mn(4)···Mn(4′) pair (Table 6) and the expected antiferromagnetic interactions. The alignment of the Mn(3) spin vec-

tor, mainly determined by its interactions with Mn(1) and Mn(2) through the hydroxo oxygen [O(22), triangular arrangement], is not clear; however, for symmetry reasons, the orientation for Mn(3) and Mn(3′) should be related by the inversion centre of the molecule, resulting in an $S = 0$ ground state.

In summary, it is tempting to assume that the $S = 0$ ground state observed for **2** arises mainly from the reasonable antiferromagnetic interaction between Mn(1) and Mn(2) [and their symmetry-related partners], assuming a strongly coupled, diamagnetic ($S_{bb} = 0$) [Mn(4)Mn(4′)-O(21)O(21′)]$^{2+}$ central subunit and excluding the possibility of spin frustration due to the asymmetry of the interactions. We would like to emphasise that this discussion is only intended to qualitatively show a possible origin of the $S = 0$ ground state observed for complex **2**.

The $S = 0$ ground state is not uncommon in octanuclear Mn clusters and has been established in [Mn$_8$O$_2$(O$_2$CEt)$_8$-(py)$_4$(L)$_2$]$^{2+}$,[6a] [Mn$_8$O$_2$(O$_2$CCH$_2$Bu^t)$_{14}$(tBuCH$_2$CO$_2$-H)$_4$][25] and [Mn$_8$O$_{10}$(O$_2$CMe)$_6$(bpy)$_2$(H$_2$O)$_2$]$^{4+}$.[28]

Complex 3

The variable-temperature magnetic-susceptibility data for compound **3** also reveal an overall antiferromagnetic behaviour. The $\chi_M T$ vs. T plot is shown in Figure 10. The value of $\chi_M T$ decreases from 12.1 cm^3·mol^{-1}·K at room temperature to 4.6 cm^3·mol^{-1}·K at 6.0 K. The room-temperature $\chi_M T$ value is slightly lower than the expected value $\chi_M T = (N\beta^2/3k)3g_i^2S_i(S_i + 1) = 13.125$ cm^3·mol^{-1}·K for three uncoupled Mn^{II} ions with $S_i = 5/2$ and $g_i = 2$ each. This value is already indicative of substantial antiferromagnetic coupling. The antiferromagnetic behaviour is further confirmed by the dramatic decrease of $\chi_M T$ when T decreases. At low temperature, the value of $\chi_M T$ almost corresponds to the expected value $\chi_M T = (N\beta^2/3k)g_i^2S(S + 1) = 4.375$ cm^3·mol^{-1}·K for an $S = 5/2$ spin state with $g = 2$.

Taking into account the molecular structure of **3**, the Kambe vector-coupling scheme shown in Figure 11 was considered. The spin Hamiltonian that describes the low-lying electronic states is given by Equation (4), where S_i is
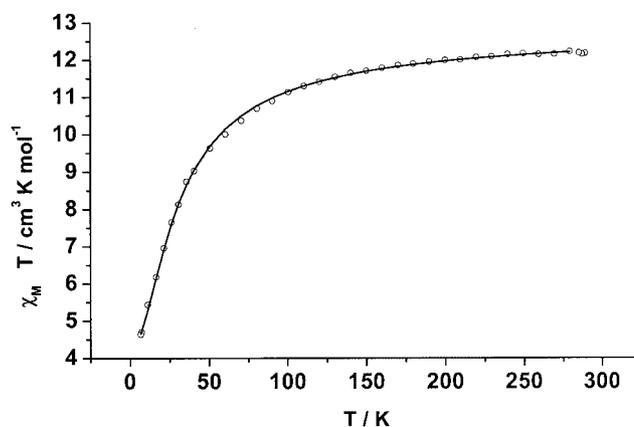

Figure 10. $\chi_M T$ vs. T plot for complex **3**; the solid line is the best theoretical fit to the data (see text for details)

the spin of the Mn^{II} ion with number i (Figure 11) and $J_{12} = J_{21'} = J$.

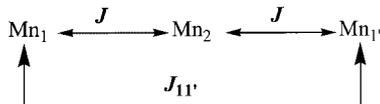$$H_s = -J(S_1 S_2 + S_2 S_{1'}) - J_{11'} S_1 S_{1'} \qquad (4)$$

Figure 11. The Kambe vector-coupling scheme used for the interpretation of the magnetic behaviour of complex **3**

The experimental data were fitted with the susceptibility expression derived from the Van Vleck formula for three $S = 5/2$ spins. The best fit was obtained for $J = -2.74$ cm^{-1}, $J_{11'} = 0.7$ cm^{-1} and $g = 1.99$. The agreement between this calculation and experimental data is excellent, as can be judged from Figure 10. The agreement factor, defined as $R = \Sigma(\chi_M^{calcd.} - \chi_M^{exp})^2/\Sigma(\chi_M^{exp})^2$ is 4×10^{-4}. The J value obtained leads to a total-spin ground state of $S = 5/2$. The system can be reasonably fitted with only one J value ($J_{11'} = 0$) but this gives a worse agreement with experimental data. We refrain from analyzing further the magnetic properties of **3**, since detailed studies are available[32a,32b,35] for trinuclear Mn^{II} carboxylate complexes with similar structures.

The J value of **3** is well within the reported range (-5.6 to -1.9) reported for other trinuclear manganese(II) complexes containing the $[Mn_3(\eta^1:\eta^1:\mu_2\text{-}O_2CR)_4(\eta^1:\eta^2:\mu_2\text{-}O_2CR)_2]^0$ core[32] (see also Table 5). This indicates that weak antiferromagnetic coupling is mediated by the bridging carboxylate groups, which is as expected, since the Mn−O distances are relatively long in such compounds.[32] J values reported in the manganese(II) literature with *only* carboxylate groups as bridging ligands are always small and negative, between approximately -0.2 and -5 cm^{-1},[13] indicating weak antiferromagnetic coupling.

Electrochemistry of Complex 2

Complex **2** was investigated by cyclic voltammetry (CV), in CH$_2$Cl$_2$, and the corresponding voltammogram is shown in Figure 12. It should be stressed at this point that there is no actual proof that complex **2** retains its structure in solution. However, the non-coordinating nature of CH$_2$Cl$_2$ and the fact that solutions of **2** in CH$_2$Cl$_2$ are non-conducting both provide strong evidence that the structure of the complex is retained in solution. The cyclic voltammogram shows only broad, irreversible features — two oxidations at about 1.24 and 0.57 V, and three reductions at -0.69, 0.06, and 0.98 V, vs. a calomel electrode (4 M KCl). Since complex **2** is valence-trapped, probably owing to the increase in the barrier to intramolecular electron transfer resulting from the JT distortion of Mn^{III},[18a] it is likely that the reduction and oxidation of **2** will be centred at particular Mn ions. It is relatively rare for high-nuclearity Mn/O/RCO$_2^-$ aggre-

gates to exhibit reversible redox processes, and thus the observed behaviour is typical of polynuclear Mn carboxylate complexes.[18a]
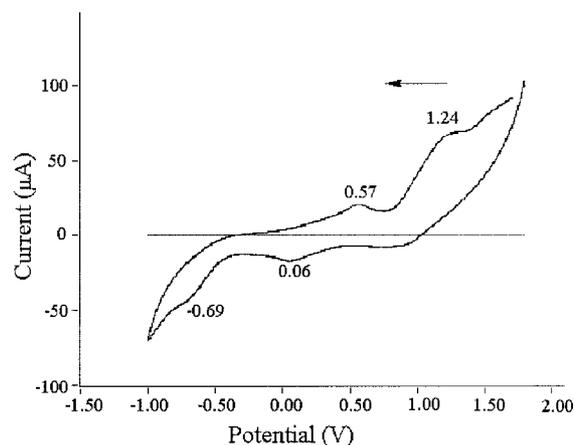

Figure 12. Cyclic voltammogram of complex **2** in CH$_2$Cl$_2$; scan rate: 100 mV s^{-1}; the potentials are given vs. a calomel electrode (4 M KCl)

Conclusions and Perspectives

The first use of (ph)(2-py)CNOH in Mn carboxylate chemistry has provided access to new complexes, one mononuclear (**1**) containing Mn^{II}, and the other octanuclear (**2**) with an unprecedented $[Mn_4^{II}Mn_4^{III}(\mu_4\text{-}O)_2(\mu_3\text{-}OH)_2]^{14+}$ core. In the former case, the ligand is neutral and chelates through its nitrogen atoms; in the latter case, the ligand is monoanionic chelating and bridging $Mn^{II}Mn^{III}$ or Mn_2^{III} pairs (Figure 4). Although the octanuclear cluster has been found to possess an $S = 0$ ground state, the bridging mode of (ph)(2-py)CNO$^-$ nevertheless suggests possibilities for other Mn_x species that might exist (e.g. clusters containing the strongly coordinating inorganic anions NO$_3^-$, N$_3^-$ and SO$_4^{2-}$) and which may have high-spin ground states. In addition, it provides encouragement for believing that a variety of carboxylate and non-carboxylate M_x^{II} and M_x^{III} clusters (M^{II} = Co^{II}, Ni^{II}; M^{III} = Cr^{III}, Fe^{III}) should also be accessible with this anionic ligand, leading to species with new topologies and exciting magnetic properties. Results with Co$^{II,II/III}$ and Ni^{II} at the time of writing reveal that the nature of (ph)(2-py)CNO$^-$ makes it a versatile ligand for a variety of objectives/advantages, including μ_2 and μ_3 behaviour, high-nuclearity cluster formation, linking of clusters into polymeric arrays, 3d-4f mixed-metal chemistry and ferromagnetic exchange interactions. Clearly, the use of other pyridyl- or polypyridyl oximes offers a potential route to other new polynuclear metal complexes, and such studies are currently under progress.

Analogues of compound **2** with acetates or substituted benzoates are not known, at least to date, and it is currently not evident whether the preparation and the stability of this Mn_8 species are dependent on the particular nature of the PhCO$_2^-$ ligand.

Complex **3** is a new addition to the growing family of trinuclear complexes with the $[M_3(\eta^1{:}\eta^1{:}\mu_2\text{-}O_2CR)_4(\eta^1{:}\eta^2{:}\mu_2\text{-}O_2CR)_2]^0$ core (M = Mn, Fe, Co), providing a useful new datum point for the ongoing objective of fully understanding the ground-state spin value of transition metal carboxylate clusters as a function of metal, oxidation state and topology of the polynuclear metal core. The structural motif of the linear trinuclear $[M_3(O_2CR)_6]^0$ unit turns out to be as important as that of the triangular basic carboxylate motif, which is characteristic of the trivalent and mixed-valent $M^{II}M_2^{III}$ analogues. Clearly, the inability of phenyl 2-pyridyl ketone, (ph)(2-py)CO, to give the *gem*-diol form [(ph)(2-py)C(OH)$_2$] in solution in the presence of metal ions, restricts its utility to the synthesis of polynuclear metal complexes, in contrast with its bis(2-pyridyl) analogue, (2-py)$_2$CO.

Experimental Section

Materials and Physical Measurements: All manipulations were performed using materials (Merck, Aldrich) as received. Compounds Mn(O$_2$CPh)$_2$·2H$_2$O,[15] N*n*Bu$_4$MnO$_4$ [14] and (N*n*Bu$_4$)[Mn$_4$O$_2$-(O$_2$CPh)$_9$(H$_2$O)][15] were synthesised according to published methods. Elemental analysis (C, H, N) were performed by the University of Ioannina (Greece) Microanalytical Laboratory using an EA 108 Carlo Erba analyzer. IR spectra (4400−450 cm^{-1}) were recorded from KBr pellets on a Perkin−Elmer PC 16 FT-IR spectrometer. Magnetic susceptibility measurements in the range of 2−300 K and magnetisation measurements (2−4 K) in the field range of 0.1−5 T for complex **2** were performed with a Quantum Design SQUID magnetometer at the Magnetochemistry Service of the University of Barcelona. Magnetic susceptibility measurements for complex **3** were performed with a DSM8 pendulum-type susceptometer operating in the range 6−300 K at magnetic fields of approximately 1 T. All measurements were performed on polycrystalline samples. Data were corrected for diamagnetic contributions calculated from Pascal constants. The cyclic voltammogram of complex **2** was recorded on a AFCBP1 Biopotentiostat and a standard three-electrode assembly (glassy carbon working, platinum wire auxiliary, SCE reference) with 0.1 M N*n*Bu$_4$PF$_6$ in distilled CH$_2$Cl$_2$ as supporting electrolyte.

[Mn(O$_2$CPh)$_2${(ph)(2-py)CNOH}$_2$]·1.2H$_2$O (1·1.2H$_2$O) and [Mn$_8$O$_2$(OH)$_2$(O$_2$CPh)$_{10}${(ph)(2-py)CNO}$_4$]·4CH$_2$Cl$_2$ (2·4CH$_2$Cl$_2$) as a Mixture: Treatment of a stirred, colourless solution of Mn(O$_2$CPh)$_2$·2H$_2$O (0.166 g, 0.50 mmol) in EtOH/MeCN (15 mL, 2:1 v/v) with solid (ph)(2-py)CNOH (0.099 g, 0.50 mmol) resulted in a pale-orange solution, which, upon slow evaporation at room temperature, turned brown due to slow oxidation of Mn^{II} under aerobic conditions. The resulting solution was evaporated to dryness under reduced pressure and the residue redissolved in CH$_2$Cl$_2$ (25 mL) to give a red-brown solution. This was layered with a mixture (50 mL, 1:1 v/v) of Et$_2$O and *n*-hexane. After several days yellow and dark-brown crystals were formed; they were carefully collected by filtration. The two products were readily separable manually, and the yellow and dark brown crystals proved by single-crystal crystallography to be complexes **1**·1.2H$_2$O and **2**·4CH$_2$Cl$_2$, respectively.

[Mn(O$_2$CPh)$_2${(ph)(2-py)CNOH}$_2$]·1.2H$_2$O (1·1.2H$_2$O): A colourless solution of Mn(O$_2$CPh)$_2$·2H$_2$O (0.166 g, 0.50 mmol) in EtOH (10 mL) was treated with solid (ph)(2-py)CNOH (0.297 g,

1.50 mmol). The solid soon dissolved. The resulting yellow solution was stirred for about 10 min and was then allowed to stand undisturbed at 5 °C for several days. Well-formed yellow crystals appeared, which were collected by filtration, washed with Et$_2$O (2 × 5 mL) and dried in air. Yields (based on Mn^{II}) as high as 0.27 g (75%) were obtained. C$_{38}$H$_{32.4}$MnN$_4$O$_{7.2}$ (715.22): calcd. C 63.8, H 4.6, N 7.8; found C 64.1, H 4.6, N 7.7. Main IR data (KBr pellet): $\tilde{\nu}$ = 3434 (m, broad), 2924 (w), 1594 (m), 1538 (s), 1468 (w), 1436 (w), 1402 (s), 1332 (w), 1256 (w), 1190 (w), 1062 (m), 1026 (m), 965 (w), 834 (w), 792 (w), 776 (w), 722 (m), 706 (m), 674 (m), 636 (w), 500 (w) cm^{-1}.

[Mn$_8$O$_2$(OH)$_2$(O$_2$CPh)$_{10}${(ph)(2-py)CNO}$_4$]·4CH$_2$Cl$_2$ (2·4CH$_2$Cl$_2$). *Method A:* Treatment of a stirred, colourless solution of Mn(O$_2$CPh)$_2$·2H$_2$O (0.166 g, 0.50 mmol) in EtOH/MeCN (15 mL, 2:1 v/v) with N*n*Bu$_4$MnO$_4$ (0.060 g, 0.16 mmol) resulted in a dark-brown solution. Solid (ph)(2-py)CNOH (0.099 g, 0.50 mmol) was slowly added to this mixture, and it soon dissolved to give a solution of essentially the same colour. The solvents were then evaporated under reduced pressure. The obtained residue was dissolved in CH$_2$Cl$_2$ (25 mL), filtered, and the filtrate layered with a mixture of Et$_2$O and n-hexane (50 mL, 1:1 v/v); slow mixing gave dark-brown crystals of the product, which were collected by filtration, washed with cold CH$_2$Cl$_2$ (2 mL) and Et$_2$O (2 × 5 mL), and dried in vacuo over silica gel. Yield (based on the oxime): 0.17 g (55%). The dried solid analysed as CH$_2$Cl$_2$-free **2**. C$_{118}$H$_{88}$Mn$_8$N$_8$O$_{28}$ (2505.66): calcd. C 56.6, H 3.6, N 4.5; found C 57.0, H 3.5, N 4.6. The crystals of **2**·4CH$_2$Cl$_2$ were found to lose solvent readily, and they were kept in the mother liquor until a suitable crystal had been found for X-ray crystallography. Main IR data (KBr pellet): $\tilde{\nu}$ = 3438 (m, broad), 3060 (w), 1596 (s), 1552 (s), 1490 (m), 1468 (m), 1444 (m), 1404 (s), 1200 (w), 1174 (w), 1110 (w), 1094 (m), 1070 (s), 1026 (m), 978 (w), 818 (w), 788 (m), 744 (w), 716 (s), 676 (s), 638 (w), 606 (m), 552 (w) cm^{-1}.

Method B: Treatment of a stirred, brown solution of (N*n*Bu$_4$)[Mn$_4$-O$_2$(O$_2$CPh)$_9$(H$_2$O)] (0.110 g, 0.07 mmol) in CH$_2$Cl$_2$ (20 mL) with solid (ph)(2-py)CNOH (0.060 g, 0.03 mmol) gave a solution of essentially the same colour. The solution was stirred vigorously for about 45 min, and layered with a mixture of Et$_2$O and *n*-hexane (40 mL, 2:1 v/v) to give X-ray quality, dark-brown crystals of **2**·4CH$_2$Cl$_2$. The crystals were collected by filtration, washed with Et$_2$O (2 × 5 mL) and dried in vacuo over silica gel. The dried solid analysed satisfactorily as **2**. The identity of the product was confirmed by IR spectroscopic comparison with the authentic sample prepared according to Method A.

[Mn$_3$(O$_2$CPh)$_6${(ph)(2-py)CO}$_2$] (3): A colourless solution of (ph)(2-py)CO (0.090 g, 0.50 mmol) in MeOH (15 mL) was added to a colourless solution of Mn(O$_2$CPh)$_2$·2H$_2$O (0.166 g, 0.50 mmol) in the same solvent (15 mL). The resulting yellow solution was stirred for 1 h. Slow evaporation of this solution at room temperature gave large yellow needles suitable for crystallography. When precipitation was judged complete, the crystals were collected by filtration, washed with Et$_2$O and dried in air. Yields (based on Mn^{II}) as high as 0.18 g (85%) were obtained. C$_{66}$H$_{48}$Mn$_3$N$_2$O$_{14}$ (1257.88): calcd. C 63.0, H 3.9, N 2.2; found C 62.7, H 3.8, N 2.2. Main IR data (KBr pellet): $\tilde{\nu}$ = 3058 (w), 1648 (m), 1606 (s), 1566 (s), 1536 (s), 1448 (w), 1400 (s), 1316 (m), 1250 (m), 1170 (m, broad), 1068 (w), 1016 (m), 952 (m), 936 (w), 858 (w), 822 (w), 768 (w), 748 (sh), 718 (s), 700 (m), 674 (m), 656 (w), 572 (wb) cm^{-1}.

X-ray Crystallographic Studies: Crystals of **1**·1.2H$_2$O and **3** were mounted in air and covered with epoxy glue, while a crystal of **2**·4CH$_2$Cl$_2$ was mounted in a capillary filled with drops of mother liquor. Diffraction measurements for **1**·1.2H$_2$O and **3** were made

Table 7. Crystal data and structure refinement for $[Mn^{II}(O_2CPh)_2\{(ph)(2-py)CNOH\}_2]\cdot1.2H_2O$ **(1·1.2H₂O)**, $[Mn_8O_2(OH)_2(O_2CPh)_{10}\{(ph)(2-py)CNO\}_4]\cdot4CH_2Cl_2$ **(2·4CH₂Cl₂)** and $[Mn_3(O_2CPh)_6\{(ph)(2-py)CO\}_2]$ **(3)**

	1·1.2H₂O	2·4CH₂Cl₂	3
Empirical formula	$C_{38}H_{32.4}MnN_4O_{7.2}$	$C_{122}H_{96}Cl_8Mn_8N_8O_{28}$	$C_{66}H_{48}Mn_3N_2O_{14}$
Mol. mass	715.22	2845.19	1257.88
Colour and habit	yellow prisms	brown prisms	yellow needles
Crystal size (mm)	$0.50 \times 0.30 \times 0.10$	$0.06 \times 0.12 \times 0.50$	$0.10 \times 0.25 \times 0.55$
Crystal system	monoclinic	monoclinic	monoclinic
Space group	$I2/a$	$C2/c$	$P2_1/a$
a (Å)	34.73(2)	32.898(8)	15.74(1)
b (Å)	10.645(5)	16.543(4)	17.29(1)
c (Å)	22.834(9)	33.206(8)	11.095(6)
α (°)	90	90	90
β (°)	107.78(2)	136.09(1)	101.75(2)
γ (°)	90	90	90
V (Å³)	8039(6)	12530(5)	2956(3)
Z	8	4	2
ρ (Mg·m⁻³)	1.182	1.508	1.413
T (°C)	25	25	25
λ (Mo-K_α) (Å)	0.71073		0.71073
λ (Cu-K_α) (Å)		1.54180	
μ (mm⁻¹)	0.377	8.544	0.700
$F(000)$	2968	5776	1290
$2\theta_{max}$ (°)	43	103	47
Index ranges (°)	$-35 \leq h \leq 34$	$0 \leq h \leq 33$	$-17 \leq h \leq 17$
	$0 \leq k \leq 10$	$0 \leq k \leq 16$	$0 \leq k \leq 19$
	$0 \leq l \leq 23$	$-33 \leq l \leq 23$	$0 \leq l \leq 12$
No. of reflections collected	4687	6602	4645
No. of indep. refls./R_{int}	4538/0.0140	6462/0.0220	4391/0.0288
Data with $I > 2\sigma(I)$	3303	4495	3132
Parameters refined	467	797	390
$[\Delta/\sigma]_{max}$	0.002	0.001	0.001
GOF (on F^2)	1.037	1.055	1.080
$R1$[a]	0.0550	0.0650	0.0508
$wR2$[b]	0.1534	0.1643	0.1242
Residuals [e·Å⁻³]	0.405/-0.270	0.646/-0.603	0.553/-0.269

[a] $R1 = \Sigma(|F_o| - |F_c|)/\Sigma(|F_o|)$. [b] $wR2 = \{\Sigma[w(F_o^2 - F_c^2)^2]/\Sigma[w(F_o^2)^2]\}^{1/2}$.

on a Crystal Logic Dual Goniometer diffractometer using graphite-monochromated Mo-K_a radiation. The X-ray data set for **2·4CH₂Cl₂** was collected on a P2₁ Nicolet diffractometer upgraded by Crystal Logic using graphite monochromated Cu-K_a radiation. Complete crystal data and parameters for data collection and refinement are listed in Table 7. Unit-cell dimensions were determined and refined by using the angular settings of 25 automatically centred reflections in the ranges $11 < 2\theta < 23°$ (for **1·1.2H₂O** and **3**) and $22 < 2\theta < 54°$ (for **2·4CH₂Cl₂**). Intensity data were recorded using the θ-2θ scan method. Three standard reflections monitored every 97 reflections showed less than 3% variation and no decay. Lorentz, polarisation and Ψ-scan absorption corrections were applied using the Crystal Logic software package.

The structures were solved by direct methods using SHELXS-86[43a] and refined by full-matrix least-squares techniques on F^2 with SHELXL-93.[43b] For all three structures, all hydrogen atoms [except those of O(1) and O(11) for **1·1.2H₂O** and the μ_3-OH⁻ hydrogen for **2·4CH₂Cl₂** which were located by difference maps and refined isotropically] were introduced at calculated positions as riding on their parent atoms. All non-hydrogen coordinated atoms of **1·1.2H₂O** were refined anisotropically. The solvate oxygen atoms were refined isotropically. Two of them were refined with occupation factors of a total sum one; the third one, sitting on an inversion centre of symmetry, was refined with a freely refined occupation factor of about 0.20. All non-hydrogen atoms of **2·4CH₂Cl₂** and **3** were refined anisotropically.

CCDC-227429 (**1·1.2H₂O**), -195209 (**2·4CH₂Cl₂**) and -227430 (**3**) contain the supplementary crystallographic data for this paper. These data can be obtained free of charge at www.ccdc.cam.ac.uk/conts/retrieving.hmtl [or from the Cambridge Crystallographic Data Centre, 12 Union Road, Cambridge CB2 1EZ, UK; Fax: +44 1223 336033; E-mail: deposit@ccdc.cam.ac.uk].

[1] [1a] T. G. Carrell, A. M. Tyryshkin, G. C. Dismukes, *J. Biol. Inorg. Chem.* **2002**, *7*, 2−22. [1b] V. K. Yachandra, K. Sauer, M. P. Klein, *Chem. Rev.* **1996**, *96*, 2927−2950.

[2] A. Zouni, H.- T. Witt, J. Kern, P. Fromme, N. Krauss, W. Sanger, P. Orth, *Nature* **2001**, *409*, 739−743.

[3] [3a] S. Wang, M. S. Wemple, J. Yoo, K. Folting, J. C. Huffman, K. S. Hagen, D. N. Hendrickson, G. Christou, *Inorg. Chem.* **2000**, *39*, 1501−1513, and references cited therein. [3b] T. Afrati, C. Dendrinou-Samara, C. P. Raptopoulou, A. Terzis, V. Tangoulis, D. Kessissoglou, *Angew. Chem. Int. Ed.* **2002**, *41*, 2148−2150, and references cited therein.

[4] [4a] D. Gatteschi, R. Sessoli, *Angew. Chem. Int. Ed.* **2003**, *42*, 268−297. [4b] G. Christou, D. Gatteschi, D. N. Hendrickson, R. Sessoli, *MRS Bull.* **2000**, *25*, 66−71.

[5] [5a] R. Sessoli, D. Gatteschi, A. Caneschi, M. A. Novak, *Nature* **1993**, *365*, 141−143. [5b] R. Sessoli, H.-L. Tsai, A. R. Schake, S. Wang, J. B. Vincent, K. Folting, D. Gatteschi, G. Christou, D. N. Hendrickson, *J. Am. Chem. Soc.* **1993**, *115*, 1804−1816.

[6] [6a] C. Boskovic, W. Wernsdorfer, K. Folting, J. C. Huffman, D. N. Hendrickson, G. Christou, *Inorg. Chem.* **2002**, *41*, 5107−5118, and references cited therein. [6b] E. K. Brechin, M. Soler, J. Davidson, D. N. Hendrickson, S. Parsons, G. Christou, *Chem. Commun.* **2002**, 2252−2253. [6c] E. K. Brechin, C. Boskovic, W. Wernsdorfer, J. Yoo, A. Yamaguchi, E. C. Sanudo, T. R. Concolino, A. L. Rheingold, H. Ishimoto, D. N. Hendrickson, G. Christou, *J. Am. Chem. Soc.* **2002**, *124*, 9710−9711. [6d] C. J. Milios, C. P. Raptopoulou, A. Terzis, F. Lloret, R. Vicente, S. P. Perlepes, A. Escuer, *Angew. Chem. Int. Ed.* **2004**, *43*, 210−212.

[7] C. Boskovic, E. K. Brechin, W. E. Streib, K. Folting, J. C. Bollinger, D. N. Hendrickson, G. Christou, *J. Am. Chem. Soc.* **2002**, *124*, 3725−3736.

[8] G. S. Papaefstathiou, S. P. Perlepes, *Comments Inorg. Chem.* **2002**, *23*, 249−274.

[9] [9a] V. Tangoulis, C. P. Raptopoulou, A. Terzis, S. Paschalidou, S. P. Perlepes, E. G. Bakalbassis, *Inorg. Chem.* **1997**, *36*, 3996−4006. [9b] V. Tangoulis, C. P. Raptopoulou, S. Paschalidou, E. G. Bakalbassis, S. P. Perlepes, A. Terzis, *Angew. Chem. Int. Ed. Engl.* **1997**, *36*, 1083−1085. [9c] A. Tsohos, S. Dionyssopoulou, C. P. Raptopoulou, A. Terzis, E. G. Bakalbassis, S. P. Perlepes, *Angew. Chem. Int. Ed.* **1999**, *38*, 983−985. [9d] G. S. Papaefstathiou, S. P. Perlepes, A. Escuer, R. Vicente, M. Font-Bardia, X. Solans, *Angew. Chem. Int. Ed.* **2001**, *40*, 884−886. [9e] G. S. Papaefstathiou, A. Escuer, R. Vicente, M. Font-Bardia, X. Solans, S. P. Perlepes, *Chem. Commun.* **2001**, 2414−2415. [9f] G. S. Papaefstathiou, A. Escuer, C. P. Raptopoulou, A. Terzis, S. P. Perlepes, R. Vicente, *Eur. J. Inorg. Chem.* **2001**, 1567−1574. [9g] N. Lalioti, C. P. Raptopoulou, A. Terzis, A. E. Aliev, I. P. Gerothanassis, E. Manessi-Zoupa, S. P. Perlepes, *Angew. Chem. Int. Ed.* **2001**, *40*, 3211−3214. [9h] G. S. Papaefstathiou, A. Escuer, M. Font-Bardia, S. P. Perlepes, X. Solans, R. Vicente, *Polyhedron* **2002**, *21*, 2027−2032. [9i] A. K. Boudalis, F. Dahan, A. Bousseksou, J.-P. Tuchagues, S. P. Perlepes, *Dalton Trans.* **2003**, 3411−3418. [9j] A. K. Boudalis, B. Donnadieu, V. Nastopoulos, J. M. Clemente-Juan, A. Mari, Y. Sanakis, J.-P. Tuchagues, S. P. Perlepes, *Angew. Chem. Int. Ed.* **2004**, *43*, 2266−2270.

[10] C. J. Milios, E. Kefalloniti, C. P. Raptopoulou, A. Terzis, R. Vicente, N. Lalioti, A. Escuer, S. P. Perlepes, *Chem. Commun.* **2003**, 819−820.

[11] C. J. Milios, C. P. Raptopoulou, A. Terzis, R. Vicente, A. Escuer, S. P. Perlepes, *Inorg. Chem. Commun.* **2003**, *6*, 1056−1060.

[12] [12a] Y. Yu. Kukushkin, A. J. L. Pombeiro, *Coord. Chem. Rev.* **1999**, *181*, 147−175. [12b] P. Chaudhuri, *Coord. Chem. Rev.* **2003**, *243*, 143−190.

[13] C. J. Milios, E. Kefalloniti, C. P. Raptopoulou, A. Terzis, A. Escuer, R. Vicente, S. P. Perlepes, *Polyhedron* **2004**, *23*, 83−95, and references cited therein.

[14] J. B. Vincent, K. Folting, J. C. Huffman, G. Christou, *Inorg. Chem.* **1986**, *25*, 996−999.

[15] M. W. Wemple, H.-L. Tsai, S. Wang, J. P. Claude, W. E. Streib, J. C. Huffman, D. N. Hendrickson, G. Christou, *Inorg. Chem.* **1996**, *35*, 6437−6449.

[16] N. C. Harden, M. A. Bolcar, W. Wernsdorfer, K. A. Abboud, W. E. Streib, G. Christou, *Inorg. Chem.* **2003**, *42*, 7067−7076.

[17] [17a] M. A. Halcrow, W. E. Streib, K. Folting, G. Christou, *Acta Crystallogr., Sect. C* **1995**, *51*, 1263−1267. [17b] A. G. Blackman, J. C. Huffman, E. B. Lobkovsky, G. Christou, *Polyhedron* **1992**, *11*, 251−255. [17c] A. R. Schake, J. B. Vincent, Q. Li, P. D. W. Boyd, K. Folting, J. C. Huffman, D. N. Hendrickson, G. Christou, *Inorg. Chem.* **1989**, *28*, 1915−1923.

[18] [18a] H.-L. Tsai, S. Wang, K. Folting, W. E. Streib, D. N. Hendrickson, G. Christou, *J. Am. Chem. Soc.* **1995**, *117*, 2503−2514. [18b] R. C. Squire, S. M. J. Aubin, K. Folting, W. E. Streib, G. Christou, D. N. Hendrickson, *Inorg. Chem.* **1995**, *34*, 6463−6471.

[19] J. B. Vincent, H.-R. Chang, K. Folting, J. C. Huffman, G. Christou, D. N. Hendrickson, *J. Am. Chem. Soc.* **1987**, *109*, 5703−5711.

[20] H. H. Thorpe, *Inorg. Chem.* **1992**, *31*, 1585−1588.

[21] H. J. Eppley, S. M. J. Aubin, W. E. Streib, J. C. Bollinger, D. N. Hendrickson, G. Christou, *Inorg. Chem.* **1997**, *36*, 109−115.

[22] J. B. Vincent, C. Christmas, H.-R. Chang, Q. Li, P. D. W. Boyd, J. C. Huffman, D. N. Hendrickson, G. Christou, *J. Am. Chem. Soc.* **1989**, *111*, 2086−2097.

[23] B. Albela, M. S. El Fallah, J. Ribas, K. Folting, G. Christou, D. N. Hendrickson, *Inorg. Chem.* **2001**, *40*, 1037−1044.

[24] For example, see: [24a] R. W. Saalfrank, N. Löw, B. Demleitner, D. Stalke, M. Teichert, *Chem. Eur. J.* **1998**, *4*, 1305−1311. [24b] R. W. Saalfrank, N. Löw, S. Trummer, G. M. Sheldrick, M. Teichert, D. Stalke, *Eur. J. Inorg. Chem.* **1998**, 559−563.

[25] C. Boskovic, J. C. Huffman, G. Christou, *Chem. Commun.* **2002**, 2502−2503.

[26] E. K. Brechin, G. Christou, M. Soler, M. Helliwell, S. J. Teat, *Dalton Trans.* **2003**, 513−514.

[27] [27a] E. Libby, K. Folting, C. J. Huffman, J. C. Huffman, G. Christou, *Inorg. Chem.* **1993**, *32*, 2549−2556. [27b] E. K. Brechin, M. Soler, G. Christou, M. Helliwell, S. J. Teat, W. Wernsdorfer, *Chem. Commun.* **2003**, 1276−1277. [27c] S. Wang, H.-L. Tsai, K. Folting, J. D. Martin, D. N. Hendrickson, G. Christou, *J. Chem. Soc., Chem. Commun.* **1994**, 671−673. [27d] V. A. Grillo, M. J. Knapp, J. C. Bollinger, D. N. Hendrickson, G. Christou, *Angew. Chem. Int. Ed. Engl.* **1996**, *35*, 1818−1820.

[28] A. J. Tasiopoulos, K. A. Abboud, G. Christou, *Chem. Commun.* **2003**, 580−581.

[29] R. E. P. Winpenny, *Adv. Inorg. Chem.* **2001**, *52*, 1−111.

[30] K. S. Hagen, T. D. Westmoreland, M. J. Scott, W. H. Armstrong, *J. Am. Chem. Soc.* **1989**, *111*, 1907−1909.

[31] [31a] M. Soler, E. Rumberger, K. Folting, D. N. Hendrickson, G. Christou, *Polyhedron* **2001**, *20*, 1365−1369. [31b] L. F. Jones, E. K. Brechin, D. Collison, A. Harrison, S. J. Teat, W. Wernsdorfer, *Chem. Commun.* **2002**, 2794−2795.

[32] [32a] V. Tangoulis, D. A. Malamatari, K. Soulti, V. Stergiou, C. P. Raptopoulou, A. Terzis, Th. A. Kabanos, D. P. Kessissoglou, *Inorg. Chem.* **1996**, *35*, 4974−4983. [32b] S. Menage, S. E. Vitols, P. Bergerat, E. Codjovi, O. Kahn, J.-J. Girerd, M. Guillot, X. Solans, T. Calvet, *Inorg. Chem.* **1991**, *30*, 2666−2671. [32c] R. L. Rardin, P. Poganiuch, A. Bino, D. P. Goldberg, W. B. Tolman, S. Li, S. J. Lippard, *J. Am. Chem. Soc.* **1992**, *114*, 5240−5249. [32d] J. B. Vincent, G. Christou, *Adv. Inorg. Chem. Radiochem.* **1989**, *33*, 197−257. [32e] R. A. Reynolds III, W. R. Dunham, D. Coucouvanis, *Inorg. Chem.* **1998**, *37*, 1232−1241. [32f] K. Tsuneyoshi, H. Kobayashi, H. Miyamae, *Acta Crystallogr., Sect. C* **1993**, *49*, 233−236.

[33] For an excellent review on trinuclear Mn complexes, see: D. P. Kessissoglou, *Coord. Chem. Rev.* **1999**, *185−186*, 837−858.

[34] For a review on the "carboxylate shift" mechanism, see: R. L. Rardin, W. B. Tolman, S. J. Lippard, *New J. Chem.* **1991**, *15*, 417−430.

[35] B. Albela, M. Corbella, J. Ribas, I. Castro, J. Sletten, H. Stockli-Evans, *Inorg. Chem.* **1998**, *37*, 788−798.

[36] Z. Sun, P. K. Gantzel, D. N. Hendrickson, *Polyhedron* **1998**, *17*, 1511−1516.

[37] I. Chadjistamatis, A. Terzis, C. P. Raptopoulou, S. P. Perlepes, *Inorg. Chem. Commun.* **2003**, *6*, 1365−1371.

[38] M. Tiliakos, P. Cordopatis, A. Terzis, C. P. Raptopoulou, S. P. Perlepes, E. Manessi-Zoupa, *Polyhedron* **2001**, *20*, 2203−2214.

[39] [39a] G. B. Deacon, R. J. Phillips, *Coord. Chem. Rev.* **1980**, *33*, 227−250. [39b] H. Sakiyama, K. Tokuyama, Y. Matsumura, H. Okawa, *J. Chem. Soc., Dalton Trans.* **1993**, 2329−2334.

[40] R. D. Cannon, R. P. White, *Prog. Inorg. Chem.* **1988**, *36*, 195−298.

[41] K. Kambe, *J. Phys. Soc. Jpn.* **1950**, *48*, 15.

[42] [42a] E. Libby, J. K. McCusker, E. A. Schmitt, K. Folting, D. N. Hendrickson, G. Christou, *Inorg. Chem.* **1991**, *30*, 3486−3495. [42b] S. Wang, K. Folting, W. E. Streib, E. A. Schmitt, J. K. McCusker, D. N. Hendrickson, G. Christou, *Angew. Chem. Int. Ed. Engl.* **1991**, *30*, 305−306. [42c] G. Aromi, S. Bhaduri, P. Artus, J. C. Huffman, D. N. Hendrickson, G. Chris-

tou, *Polyhedron* **2002**, *21*, 1779−1786. [42d] C. Cañada-Vilalta, J. C. Huffman, G. Christou, *Polyhedron* **2001**, *20*, 1785−1793.

[43] [43a] G. M. Sheldrick, *SHELXS-86*, Program for the Solution of Crystal Structures, University of Göttingen, Germany, **1986**. [43b] G. M. Sheldrick, *SHELXL-93*, Program for the Refinement of Crystal Structures, University of Göttingen, Germany, **1993**.